

TECHNICAL REPORT BRL-TR-2973

BRL

1938 - Serving the Army for Fifty Years - 1988

STUDIES OF THE EFFECT OF HIVELITE AND OTHER
BORON COMPOUNDS ON NITRAMINE DECOMPOSITION
BY PYROLYSIS GC-FTIR

S DTIC
ELECTE **D**
APR 10 1989
D ²

PAMELA J. KASTE

DECEMBER 1988

APPROVED FOR PUBLIC RELEASE, DISTRIBUTION UNLIMITED.

U.S. ARMY LABORATORY COMMAND

BALLISTIC RESEARCH LABORATORY
ABERDEEN PROVING GROUND, MARYLAND

DESTRUCTION NOTICE

Destroy this report when it is no longer needed. DO NOT return it to the originator.

Secondary distribution of this report is prohibited.

Additional copies of this report may be obtained from the Defense Technical Information Center, Cameron Station, Alexandria, VA 22314.

The findings in this report are not to be construed as an official Department of the Army position, unless so designated by other authorized documents.

The use of trade names or manufacturers' names in this report does not constitute indorsement of any commercial product.

REPORT DOCUMENTATION PAGE

Form Approved
OMB No. 0704-0180

1a. REPORT SECURITY CLASSIFICATION Unclassified		1b. RESTRICTIVE MARKINGS	
2a. SECURITY CLASSIFICATION AUTHORITY		3. DISTRIBUTION/AVAILABILITY OF REPORT APPROVED FOR PUBLIC RELEASE; DISTRIBUTION UNLIMITED.	
2b. DECLASSIFICATION/DOWNGRADING SCHEDULE		5. MONITORING ORGANIZATION REPORT NUMBER(S)	
4. PERFORMING ORGANIZATION REPORT NUMBER(S) BRL-TR-2973		7a. NAME OF MONITORING ORGANIZATION	
6a. NAME OF PERFORMING ORGANIZATION US Army Ballistic Research Laboratory	6b. OFFICE SYMBOL (If applicable) SLCBB-IB	7b. ADDRESS (City, State, and ZIP Code)	
6c. ADDRESS (City, State, and ZIP Code) Aberdeen Proving Ground, MD 21005-5066		9. PROCUREMENT INSTRUMENT IDENTIFICATION NUMBER	
8a. NAME OF FUNDING/SPONSORING ORGANIZATION	8b. OFFICE SYMBOL (If applicable)	10. SOURCE OF FUNDING NUMBERS	
8c. ADDRESS (City, State, and ZIP Code)		PROGRAM ELEMENT NO. 61102A	PROJECT NO. AH43
11. TITLE (Include Security Classification) STUDIES OF THE EFFECT OF HIVEHITE AND OTHER BORON COMPOUNDS ON NITRAMINE DECOMPOSITION BY PYROLYSIS GC-FTIR		TASK NO.	WORK UNIT ACCESSION NO.
12. PERSONAL AUTHOR(S) Pamela J. Kaste			
13a. TYPE OF REPORT Final	13b. TIME COVERED FROM Jan 85 TO Aug 86	14. DATE OF REPORT (Year, Month, Day)	15. PAGE COUNT
16. SUPPLEMENTARY NOTATION <i>continued on p. 9</i> <i>Keywords continued</i>			
17. COSATI CODES		18. SUBJECT TERMS (Continue on reverse if necessary and identify by block number)	
FIELD	GROUP	RDX, HMX, Hivelites, TAGN, Thermal Analysis, FTIR, Pyrolysis GC	
09	01		
07	03		
19. ABSTRACT (Continue on reverse if necessary and identify by block number)			
<p>The role of borohydride compounds in very high burning rate (VHBR) materials has been studied using two nitramines (cyclotrimethylene trinitramine, or RDX, and cyclotetramethylene tetranitramine, or HMX) and three boron compounds (the potassium and tetramethylammonium salts of the $B_{12}H_{12}^{-2}$ anion and $NaBH_4$). Pyrolysis products of these materials have been separated by capillary gas chromatography, GC, and characterized by Fourier transform Infrared (FTIR) spectroscopy. Two-component and three-component nitramine/borohydride combinations, as well as pressed propellant formulations previously tested in the closed bomb, have been studied in order to determine which reaction products of the nitramines are modified by the boron compounds. In addition to the permanent gas products typically observed, larger molecular weight species including amides and nitroso compounds have been identified. The product distributions suggest that the rate of energy release is greater in the nitramine/boron systems than that of either borohydride or nitramine alone, and that decomposition occurs at a lower temperature in the</p>			
20. DISTRIBUTION/AVAILABILITY OF ABSTRACT <input type="checkbox"/> UNCLASSIFIED/UNLIMITED <input checked="" type="checkbox"/> SAME AS RPT <input type="checkbox"/> DTIC USERS		21. ABSTRACT SECURITY CLASSIFICATION Unclassified	
22a. NAME OF RESPONSIBLE INDIVIDUAL DR. PAMELA J. KASTE		22b. TELEPHONE (Include Area Code) 301-278-6168	22c. OFFICE SYMBOL SLCBB-IB-P

19. Abstract (Cont'd):

Nitramine/borohydride mixtures than with the nitramine alone. These conclusions are also supported by DSC results. *Keywords, do as title*
Previous page

TABLE OF CONTENTS

	<u>Page</u>
LIST OF FIGURES.....	5
LIST OF TABLES.....	7
I. BACKGROUND.....	9
II. INTRODUCTION.....	9
III. EXPERIMENTAL.....	10
A. Instrumentation.....	10
B. Materials.....	13
C. Procedure.....	13
D. Results.....	15
IV. RDX AND HMX MIXES WITH BOROHYDRIDE SALTS.....	22
V. PYROLYSIS PRODUCT ANALYSIS BY PACKED COLUMN CHROMATOGRAPHY.....	26
VI. THERMAL ANALYSIS RESULTS.....	28
VII. DISCUSSION.....	35
ACKNOWLEDGEMENT.....	40
REFERENCES.....	41
LIST OF ACRONYMS.....	43
DISTRIBUTION LIST.....	45

Accession For	
NTIS CRA&i	<input checked="" type="checkbox"/>
DTIC TAB	<input type="checkbox"/>
Unannounced	<input type="checkbox"/>
Justification	
By	
Distribution /	
Availability Codes	
Dist	Avail and/or special
A-1	



LIST OF FIGURES

<u>Figure</u>		<u>Page</u>
1	Schematic of the Pyroprobe-Concentrator-GC-FTIR Interface.....	11
2	A Typical GC/FTIR Light Pipe.....	14
3	FID and Infrared Chromatograms for the Pyrolysis Products of RDX (A) and HMX (B) at Temperatures Just Above Their Melting Point and at 800°C.....	16
4	Infrared Spectra of Components Seen in the Low Temperature Decomposition of HMX (320°C) and RDX (280°C).....	17
5	Infrared Spectrum of a Low Temperature (320°C) Decomposition Product of HMX.....	18
6	Molecular Structures of Compounds/Functional Groups Observed in RDX Decomposition.....	19
7	Infrared Spectra of Two Products Seen in the High Temperature (800°C) Decomposition of RDX and HMX.....	21
8	Infrared Spectra of Products Unique to Nitramine/Boron Mixtures.....	23
9	Infrared Chromatogram of Two Similar Propellant Formulations, TC016 (a) and TC014 (b).....	25
10	Infrared Spectra of Two Decomposition Products Isolated in the Packed Column Analysis and not Seen in the Concentrator-Capillary Work.....	29
11	DSC Results for RDX (a) and Roughly 50:50 Mixtures of RDX with the Potassium Boron Salt (b), the TSA Boron Salt (c) and NaBH_4 (d).....	30
12	DSC Results for the Potassium Dodecahydrododecaborane (a) and Tetramethylammonium Dodecahydrododecaborane (b) Salts.....	32
13	TGA Results for the Potassium Boron Salt (a) and the TSA Boron Salt (b).....	33
14	DSC Results for Mixtures of RDX with Elemental Boron (a), the TSA Salt Pretreated at 460°C (b) and 760°C (c).....	34

LIST OF TABLES

<u>Table</u>	<u>Page</u>
1	Pyrolysis and Chromatographic Conditions Used in Decomposition Experiments.....12
2	Gas Chromatographic Retention Times and Infrared Vapor Phase Frequencies for the Compounds Found in Pyrolysis- GC FTIR Studies.....20
3	Formulations of the Propellants Studied by Pyrolysis- GC-FTIR, Chosen Because Previous Studies Were Performed On These Using a Closed Bomb.....24
4	Summary of Compounds Found in Each Sample Pyrolyzed and Analyzed by Capillary GC-FTIR.....26
5	Summary of Compounds Found in Each Sample Pyrolyzed and Analyzed by Packed Column GC-FTIR.....28

I. BACKGROUND

The traveling charge gun propulsion concept is being explored at the Ballistic Research Laboratory. A traveling charge is one in which the propellant is attached to the projectile, and for which burning rates in the range of 100-500 m/s are required. Most very high burning rate (VHBR) formulations investigated contain $B_{10}H_{10}^{-2}$ salts called Hivelites which are marketed by Teledyne McCormick-Selph. These hydrides were chosen because of their reported ability to cause burning rates intermediate between deflagration and detonation in previously prepared formulations. However, little is known of the chemical mechanisms by which these materials accelerate propellant burning rates. Also, such high burning rates are due, in part at least, to physical characteristics of the traveling charge propellants. In a study by Juhasz, et al.,¹ both chemical and physical parameters were varied in order to develop guidelines for future formulations. In a series of formulations in which the binder, density and composition was altered, it was found that increasing the solids loading or porosity of otherwise similar propellant formulations increased the burning rate.

In another phase of the same study,¹ chemical effects were investigated. The crystalline oxidizer (RDX, HMX, or triaminoguanidine nitrate, TAGN) was varied and the effect of adding/changing borohydride was also explored. The maximum burning rate achieved was 250 m/sec, well within the range needed for the traveling charge program. The possibility of attaining VHBR characteristics using only organic (C/H/N/O) compounds was tested by preparing samples of porous consolidated ball powder. The burning rates were much lower with an average of 3-4 m/s, although it was assumed that somewhat higher rates could be achieved by improving sample preparation techniques. Thus, it appears that the Hivelite is an essential ingredient in achieving VHBR behavior in the current formulations.

The above studies showed that physical characteristics of the traveling charge propellants affect the burning rates considerably, as does the presence of Hivelite. Thus, the extent to which the chemistry of the boron hydrides is responsible for the increased burning rate is unclear. Although the boron hydride seems to be essential for achieving VHBR behavior, the chemical mechanism is not known, and several theories have been proposed concerning the roles of hydrogen atoms/ions in the combustion process.² A simple boron compound, $NaBH_4$ has been shown to accelerate nitramine combustion.^{3,4} In this work $NaBH_4$ has been studied in an attempt to determine if other boron materials may undergo similar reactions and may also have potential for improved ballistic performance. $B_{12}H_{12}$ salts marketed by Callery Chemical, have also been studied in the closed bomb and acceptable burning rates were obtained. These salts have been studied in this work.

II. INTRODUCTION

The goal of this work is to determine which pyrolysis products of the nitramines (RDX and HMX) are modified by the presence of the borohydride materials. Such pyrolysis product information will be used to determine basic chemical reactions/interactions between the Hivelites and nitramines which could ultimately be useful in understanding Hivelite burning rate promotion. However, a more immediate benefit could be the correlation of product concentration with the larger-scale lab tests such as the closed bomb.

Pyrolysis-GC has previously been used in basic research studies of combustible materials and has been shown to be a useful tool for predicting large scale behavior from smaller scale analyses.⁵ Pattern recognition techniques are often used to predict experimental properties from the many and complex chromatograms generated in pyrolysis GC-FTIR experiments.⁶ In order to predict experimental products, two classes of samples are usually studied: a class exhibiting a specific experimentally tested property and a class which either does not exhibit or exhibits an unacceptable level of the property. Often a desirable and an undesirable class is obtained, e.g., healthy vs. diseased. In this work, the measured property of interest, a "very high burning rate", would form one class and an unacceptably high burning rate would form the other. Products from each class of samples are determined and trends or patterns in the data are sought. That is, differences in the products or levels of products seen in one class but not the other are identified and used as markers to predict the classification of unknown samples. Such predictions could facilitate the testing of future propellant formulations for "very high burning rates".

In order to obtain mechanistic or classification information it is essential to have carefully controlled, reproducible pyrolysis experiments in which decomposition products are generated which enable mechanisms/correlations to be drawn. There has been much research in the area of nitramine pyrolysis and reaction mechanism determination, however, most papers report final product-type compounds such as the permanent gases.⁷ This is due to the difficulty in stopping or quenching propellant decomposition once it begins.

From small "final product" type compounds it is difficult to derive mechanisms and correlations. However, a concentrator-pyrolysis system has enabled the generation of larger molecular weight products which make mechanistic and correlation studies more feasible. Separation and detection of these products is achieved using gas chromatography and a flame ionization detector (FID) detector. The interfacing of an FTIR detector to the system enables identification of the RDX and/or borohydride pyrolyzates, many of which, to this author's knowledge, have not been previously reported in nitramine pyrolysis. The system is described in detail in the experimental section.

III. EXPERIMENTAL

A. Instrumentation:

The instrumentation schematic for this work is shown in Figure 1. The experiment can be thought of as consisting of three steps. In the first step the samples are pyrolyzed using Chemical Data Systems (CDS) pyrolysis/concentrator equipment. Next, the samples are separated using a gas chromatograph with FID and finally the components are identified by FTIR. The details are given below.

The samples are pyrolyzed in a CDS L20 Pyroprobe which consists of a resistively heated coiled wire in which the final temperature, heating rate and duration can be controlled. Samples were prepared by placing about 1 mg of the powdered material in a quartz tube, nominally 2.6 cm and 0.2 cm ID; the sample is sandwiched between two quartz wool plugs so that only the vapor

Instrumentation Schematic

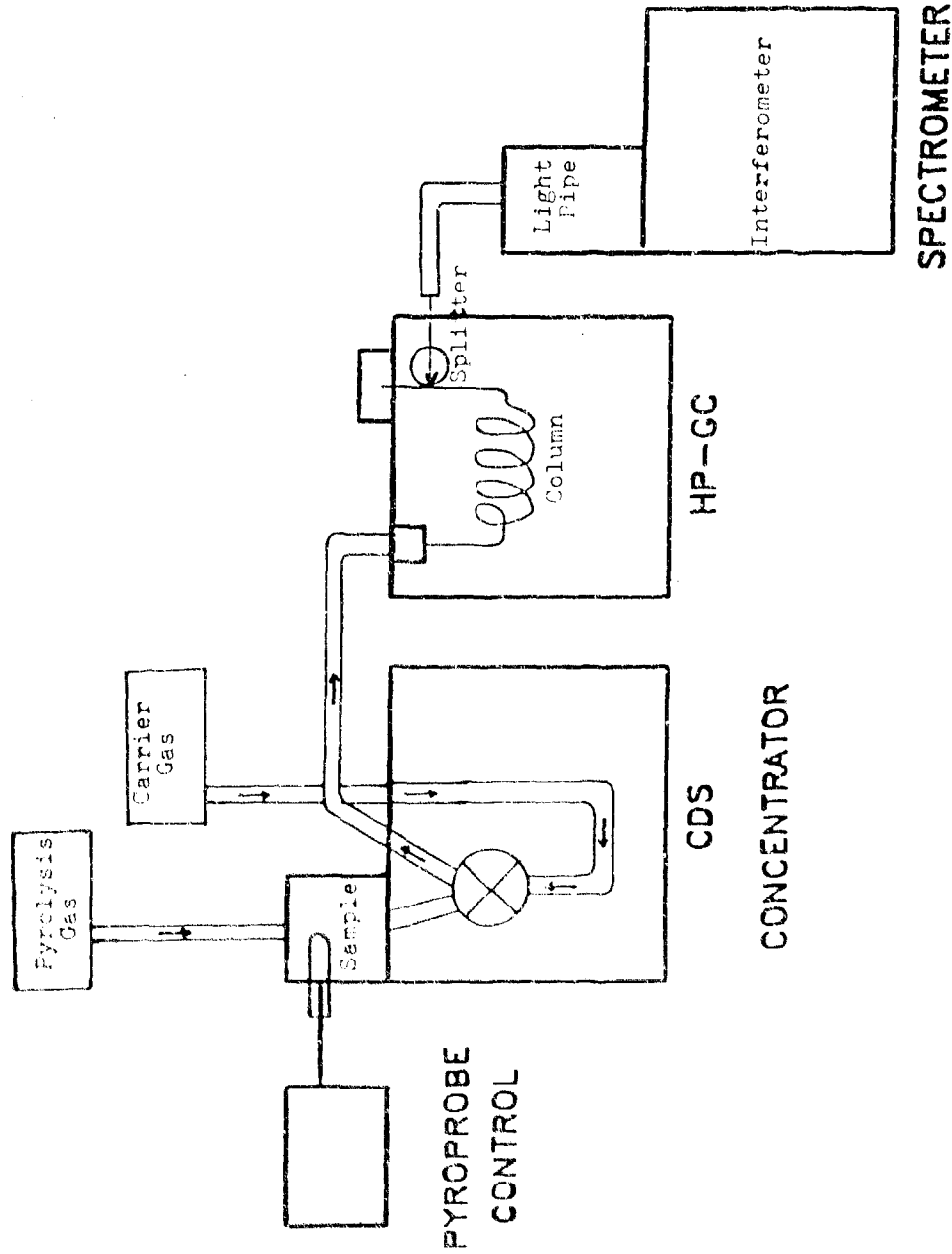


Figure 1. Schematic of the Pyroprobe-Concentrator-GC-FTIR Interface. The eight port valve controls the flow of the pyrolysis products. In position 1 the products are swept onto trap A by the carrier gas; in position 2, trap A is backflushed with carrier gas and the volatiles are chromatographed and analyzed by FTIR spectroscopy.

phase decomposition products were swept from the tube. The tube is inserted into the center of the coiled wire of the probe and this assembly is inserted into the pyrolysis interface of the CDS 330 concentrator. The interface temperature is also programmable and the ports in the interface allow the user to admit any pyrolysis atmosphere desired. In this work helium was used, although reactive gases could be used as well. The temperature and flow rate of the gas over the sample is also programmable. The careful control of all these pyrolysis parameters enables one to obtain reproducible results not often achieved in other pyrolysis systems.

The samples were pulse heated in the coil probe to their final temperature and held for 20 seconds. Helium (0.14 MPa or 20 psi) was used as the pyrolysis atmosphere as well as the GC carrier gas. The pyrolysis gas sweeps the sample onto a trap in the concentrator unit. The trap may be packed with a porous packing material or it may be empty, in which case the samples are cryogenically trapped. The pyrolysis products are held on the trap for the duration of the pyrolysis event. Smaller molecular weight gases such as NH_3 , HCN, and N_2O eluted through the trap heated and are not detected. The trap is then backflushed with the GC carrier gas and transferred via a heated line (1.5 m, 210°C) to the interface at the head of the column where the samples are cryofocused (-30°C) to ensure high chromatographic resolution. It should be noted that the entire pyrolysis/concentrator system is glass lined, so that metal catalysis/interference is avoided. After a one minute delay the column is heated from 30°C to 200°C at 30 deg/min. The separations were achieved using a Hewlett Packard 5840A GC with a Quadrex OV-17 (25m, 0.35 mm ID, 3.0 μ film thickness fused silica column with He at a head pressure of 0.14 MPa (20 psi). The components were detected with the standard flame ionization detector (FID). The pyrolysis and chromatographic conditions used in this study are listed in Table I.

Table I. Pyrolysis and Chromatographic Conditions Used in Decomposition Experiments

Pyrolysis

Probe Temperature:	280°C (RDX samples), 320°C (HMX samples), 800°C (all samples)
Desorb Heater:	200°C
Trap A:	-30°C initial temperature, all samples run on both empty and Tenax traps
Transfer Line:	210°C
Valve Oven:	210°C

Chromatography

Program:	30°C for 1 min, then 20°C/min to 230 for 24 min
Column:	Quadrex OV-17 (25 m, 0.35 mm ID, 3 μ film Poropak N Co. II, 1/8 in, 80-100 mesh)

As the samples elute from the capillary column they are split approximately 1:20 using a Scientific Glass and Engineering (SGE) splitter. The larger portion passes through a second heated transfer line (also 1.5 m, 210°C) into the light pipe necessary at the FID. This accessory is mounted

onto the side of the FTIR spectrometer and receives the external beam via an automatic mirror flipper (controlled by the software). The accessory consists of a set of optics which focuses the IR beam into the heated light pipe (240°C). The chromatographic effluent continuously passes through the light pipe and spectra of the separated components are obtained on-the-fly. A schematic of the light-pipe is shown in Figure 2. It consists of a gold-coated glass tube with infrared-transmitting KBr windows at each end. The IR source radiation passes through the windows and makes multiple reflections down the tube through which the gas continuously passes. An eight wavenumber spectrum is obtained in slightly less than a second so that about 10 scans can be signal averaged for a seven second peak.

The Digilab software monitors the total IR absorption at the detector as a function of time which yields an IR "chromatogram" analogous to the flame ionization chromatogram. Typically fewer peaks are observed in the IR because some components are not IR-absorbing, whereas the FID is fairly universal for organic compounds. Also, the infrared is about 2 orders of magnitude less sensitive than the FID. However, the IR offers identification information not obtainable with the FID. This is done by selectively co-adding points within each peak in the IR chromatogram. Individual points in an FTIR peak were co-added so that about 80% of the points, centered about the maximum, were included. Exceptions to this procedure occurred if the peaks were overlapped or consisted of more than one component as evidenced by different relative band intensities in points across the peak.

Differential scanning calorimetry results were obtained using a DuPont Model 910 calorimeter with helium as a purge gas with a flow of 30 cc/min. Samples, nominally 2 mg, were run in open pans. The heating rate was 20°C/min from 30°C to 460°C. TGA results were obtained with a 951 thermogravimetric analyzer. A DuPont 1090 thermal analyzer was used for data analysis.

B. Materials:

Samples of the $B_{12}H_{12}$ salts were obtained from Gallery Chemical Company. Military grade RDX and HMX were recrystallized from acetone. $NaBH_4$ was obtained from Ventron, Alfa Division. Samples were pyrolyzed with an interface heater setting of 200°C.

C. Procedure:

Smaller, more common (and possibly more stable) species were identified by comparison of their spectra to recorded spectra; however, a few pyrolyzates could be identified only with respect to functional groups present. This is due in part to the generation of intermediate-type products not typically found in infrared libraries, and to the fact that infrared vapor phase libraries are much more limited (and expensive) than are condensed phase libraries. An EPA vapor phase library consisting of about 2800 compounds and available through Digilab was used to search selected spectra and although an exact match was not always available, such searching was useful for classifying compounds according to the functional groups present. The number of closest hits reported is pre-selected by the operator, and a hit quality index (HQI), ranging from zero to one, is given for each hit. Zero represents a perfect match and unity indicates that no match criteria was fulfilled.

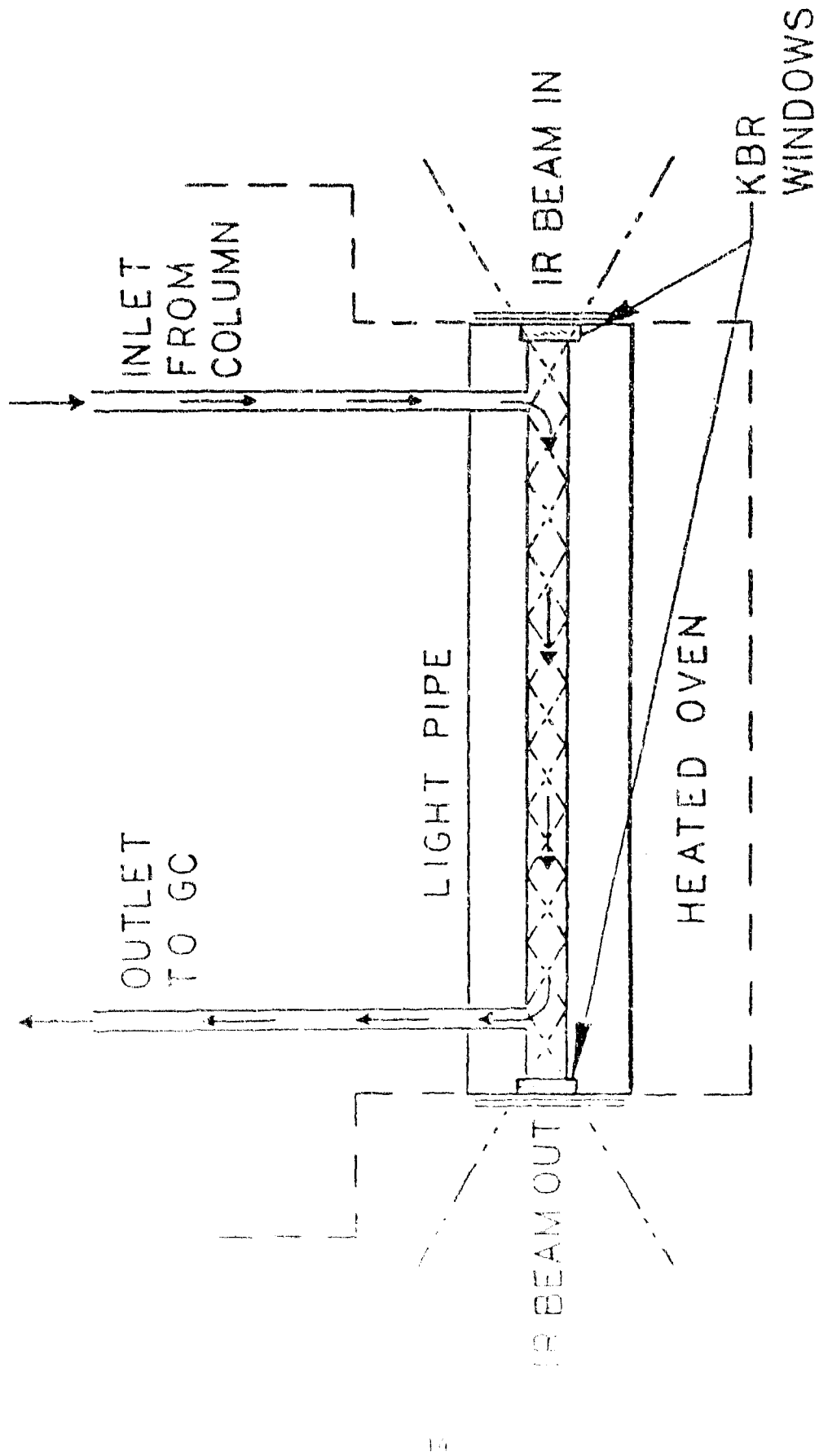


Figure 2. A Typical GC/FTIR Light Pipe

Thus, compounds with low HQI's are probably similar in structure to the recorded spectrum or contain similar functional groups.

Another identification tool, PAIRS,⁸ is available for vapor phase (as well as condensed phase) functional group identification. In this program the user is prompted with questions about the unknown spectrum inquiring about sample form, peak intensities, shape and position, and a search on the many functional groups represented in the program is run. The output consists of a pre-selected number of best match functional groups with a corresponding hit list. Although the functional groups represented are extensive, several of the materials generated in this work are probably complex urea-amide type functions which did not produce many good matches.

Finally, it should be noted that vapor phase spectra often appear quite different from conventional condensed phase spectra and this makes exact identification difficult. This is especially true for groups which can hydrogen bond, since such weak forces are not so important in the gas phase. Bands due to hydrogen-bonded groups can shift significantly (shifts up to 30-50 wavenumbers are quite common and up to 80 wavenumbers have been observed in some carbonyls). In general, peak shape and relative intensity can vary appreciably as well. However, a compilation of some general trends concerning various IR functional group positions is available which is useful in identifying many compounds.⁹

Individual components were pyrolyzed at two temperatures. RDX and HMX were pyrolyzed at coil "set" temperatures of 280 and 320°C respectively, although the samples were actually slightly above their melting points (about 205°C for RDX and 280°C for HMX). The borohydride compounds were pyrolyzed at both these temperatures, however no significant difference was evident in the products obtained regardless of which was used. Nitramine/borohydride mixtures containing HMX or RDX were pyrolyzed at 320 and 280°C, respectively. Triazine was decomposed as a reference spectrum, at both lower temperatures and at 800°C.

D. Results:

Two-component mixtures of each nitramine with each boron compound were prepared. Every individual component and mixture was also pyrolyzed at 800°C. Typical FID chromatograms and IR spectrograms of RDX and HMX are shown in Figure 3. At the low temperatures fewer peaks are seen in both the FID chromatograms and IR chromatograms than at 800°C. Infrared spectra of components seen with both RDX and HMX in low temperature decomposition are shown in Figure 4, while a single component unique to HMX is shown in Figure 5.

The compounds observed in the RDX decomposition include one with a C-nitroso functionality (a), formic acid (b), and a conjugated C=N compound (c). The latter is also seen in the decomposition of triazine ($C_3N_3H_6$), which is an analog of benzene in which alternate carbon atoms are replaced by nitrogen. In addition, formamide (d) and probably some sort of ketone (e) were also observed. (See Figure 6 for structures.) Formic acid and formaldehyde were identified by comparison to reference vapor spectra. In general, the C-nitroso functionality has a rather distinctive pattern with bands in the 1620-1540 cm^{-1} region due to the C-N=O vibration and a strong 1100-1140 cm^{-1}

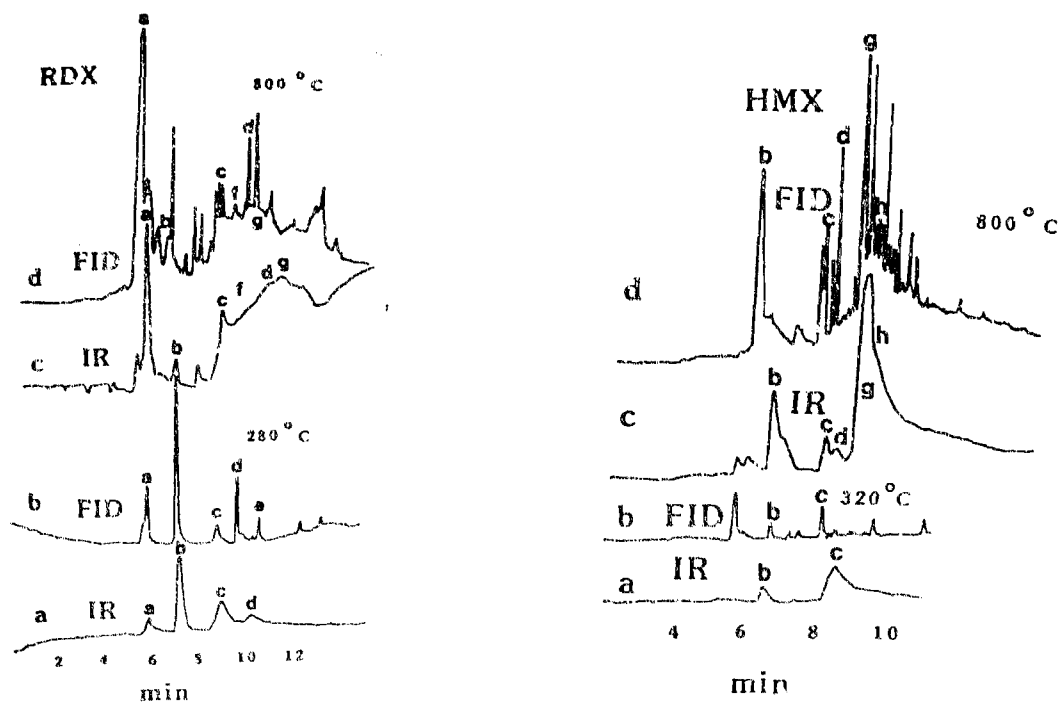


Figure 3. PID and Infrared Chromatograms for the Pyrolysis Products of RDX (A) and HMX (B) at Temperatures Just Above Their Melting Point and at 800°C.

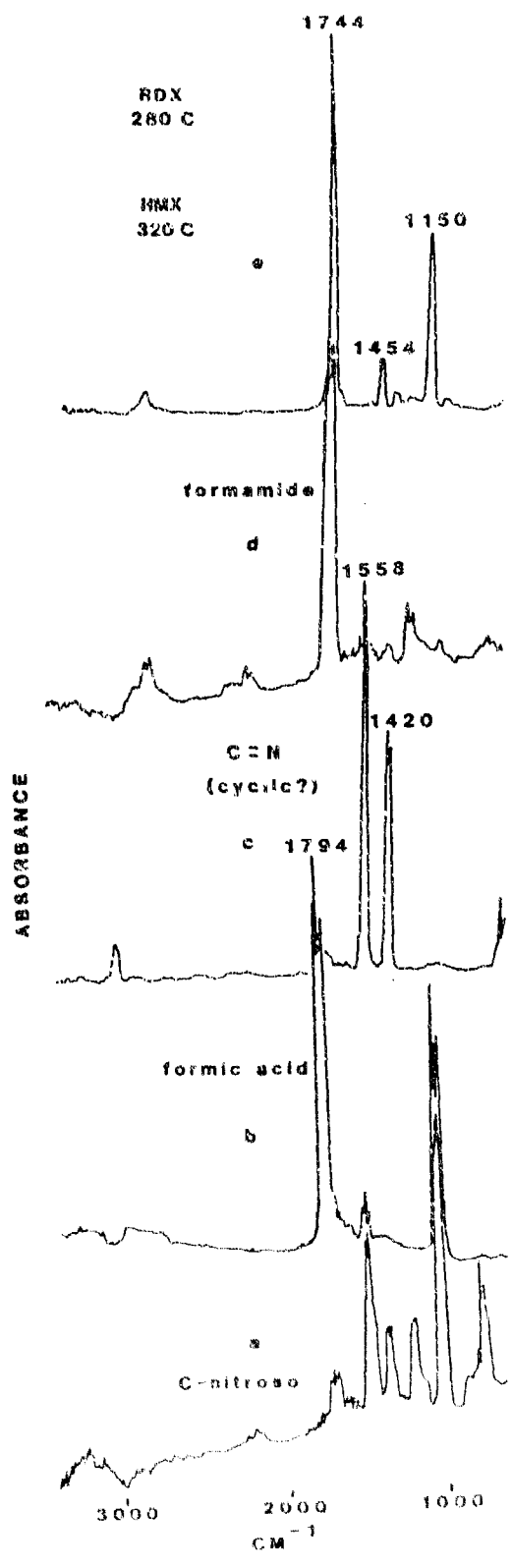


Figure 4. Infrared Spectra of Components Seen in the Low Temperature Decomposition of HMX (320°C) and RDX (280°C)

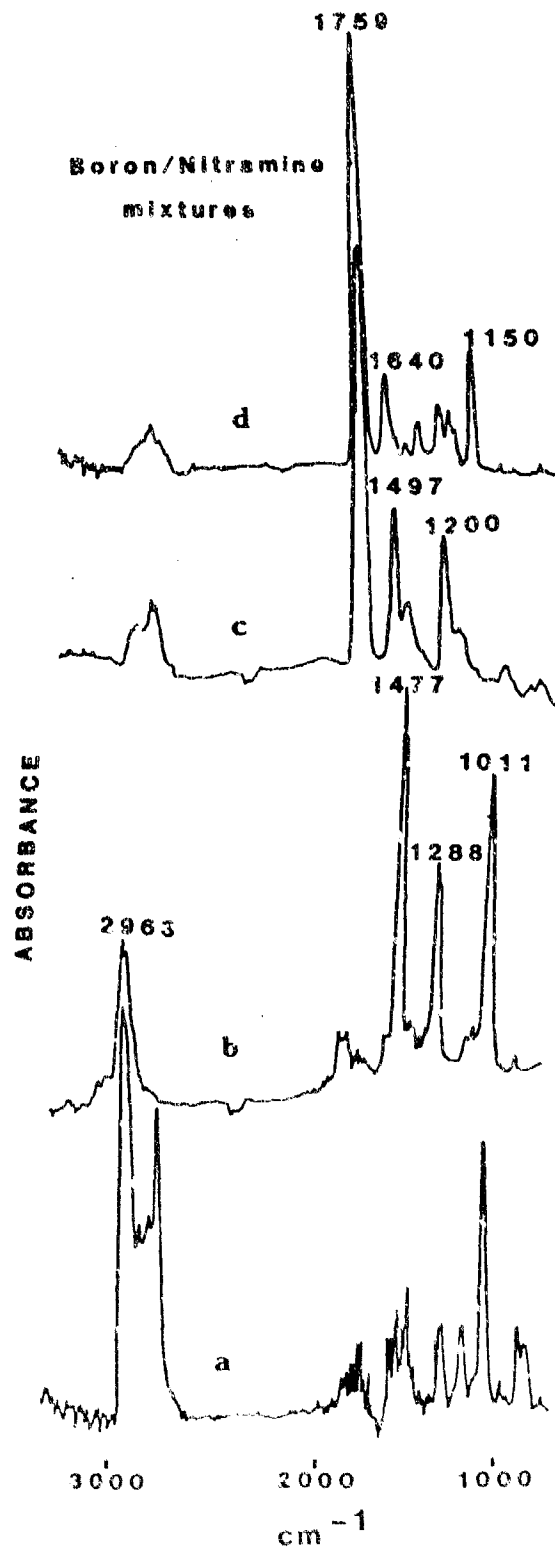


Figure 5. Infrared Spectrum of a Low Temperature (320°C) Decomposition Product of HMX

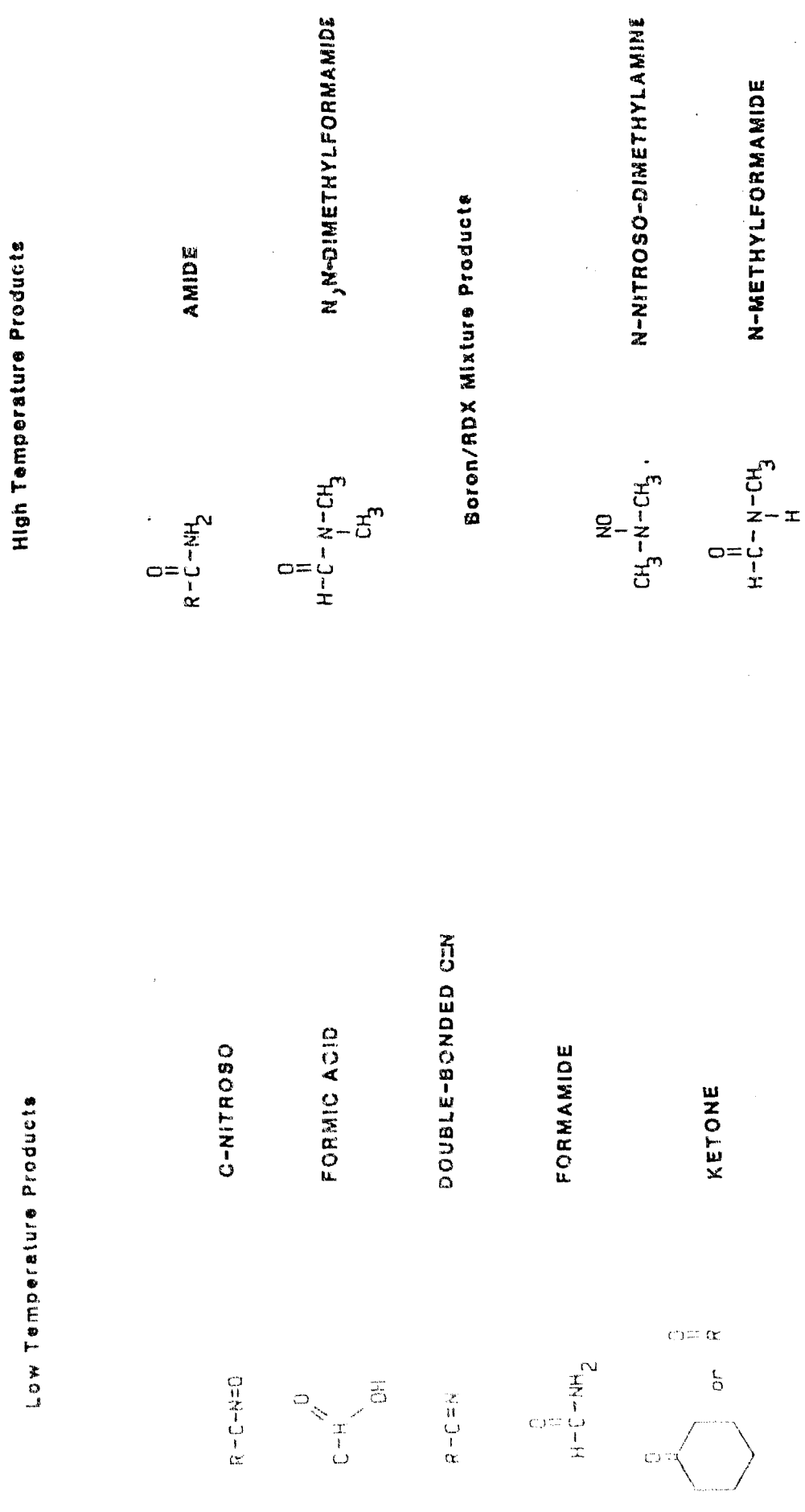


Figure 6. Molecular Structures of Compounds/Functional Groups Observed in RDX Decomposition

peak due to the C-N=O with smaller bands near 1300 and 1420 cm^{-1} . The presence of all these bands strongly supports this assignment.

Product "c" was found not only in nitramine decomposition, but with triazine as well. A conjugated C=N band would yield the two prominent bands seen in "c" and the fact that this is found in the decomposition of triazine suggests this. Speculations that this might be a nitro compound are dismissed, since no oxygen is available in the system when triazine is decomposed. Spectral searching of "e" indicates a ketone functionality, as do comparisons with ketone vapor reference spectra, but there are not enough bands to permit any further identification. The similarity of this spectrum to that of 1 cyclopenta-3-one is striking, and suggests that the ketone may be cyclic.

Formamide and the conjugated C=N (c) are consistently observed in both low and high temperature RDX/HMX decomposition while the C-nitroso, formic acid and possible ketone compounds are usually seen in lower levels, if at all, in the higher temperature decomposition. Two other products are seen only in high temperature RDX decomposition (Figure 7). The first (a) is tentatively identified as an amide whereas the second (b) gave an excellent spectral match with N,N-dimethylformamide. A list of the decomposition products and their corresponding retention times and major infrared bands is given in Table 2.

Table 2. Gas Chromatographic Retention Times and Infrared Vapor Phase Frequencies for the Compounds Found in Pyrolysis-GC FTIR Studies

<u>Compound</u>	<u>Retention Time (min)</u>	<u>IR Frequencies</u>
<u>Nitramine (low T)</u>		
C-N=O	6.5	1592/1569 1317 1134/1119 915
Formic Acid	7.2	1794/1755 1123 1084
C=N	7.7	3090 1558 1420/1400
Formamide	10.2	1771/1732 1269/1234
Ketone	11.6	1744 1150
<u>Nitramine (800°C)</u>		
Amide	9.2	3534 1798 1589 1396 1260 1175
N,N-Dimethylformamide	10.0	2936 1713 1389 1277 1080
<u>Borohydride Mixes</u>		
N-Nitrosodimethylamine	8.9	2959 1477 1288 1011
N-Methylformamide	9.4	2936/2851 1724 1381 1080
Possible Amide	6.0	2960 1771 1558 1300

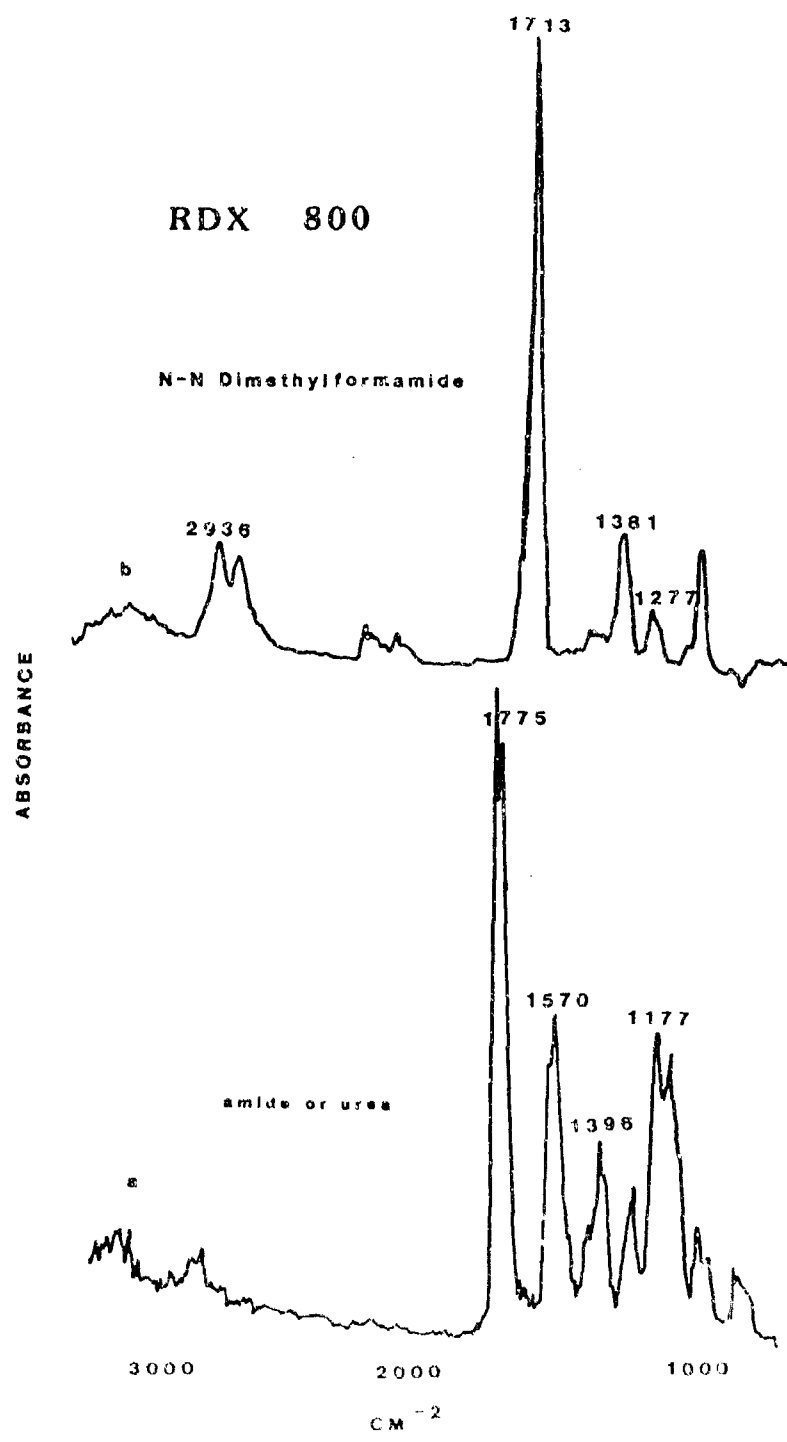


Figure 7. Infrared Spectra of Two Products Seen in the High Temperature (800°C) Decomposition of RDX and HMX

IV. RDX AND HMX MIXES WITH BOROHYDRIDE SALTS

In order to determine the effect of boron hydrides on HMX and RDX decomposition, mixtures of each nitramine with each borohydride were prepared. These samples were approximately 50:50 by weight mixtures of the nitramine and boron materials and the samples were run at both the lower (280°C for RDX and 320°C for HMX) and higher (800°C) temperatures. Each boron compound was run alone at each temperature to determine its decomposition products.

Both temperatures were studied to determine if either might correlate with trends observed in the closed bomb data. The lower temperature is of interest because it is the regime in which the nitramines begin to decompose. A significant amount of energy thus becomes available to trigger further reaction, with a corresponding increase in pressure. Minor changes in temperature/pressure around the melting point can result in significant differences in the products obtained. The lower temperature reaction is most probably indicative of what occurs very early in decomposition. It was of interest to determine if these very early events might influence and be related to the results obtained in the closed bomb studies.

When decomposed in He at 800°C the tetramethylammonium (TMA) salt yields the product spectrum shown in Figure 7a; NaBH_4 and the potassium salt gave no infrared-active products under the same conditions. None of the salts alone yielded decomposition products at the lower temperatures. The boron/nitramine mixtures revealed several decomposition products not seen with either the borohydrides or nitramines alone. The effects were the same regardless of which boron salt was used. These are shown in Figure 8b-d and include N-nitrosodimethylamine (b), N-methylformamide (c) and, most likely, another amide (d) (see Figure 6 for structures and Table 2 for the retention times and major infrared bands.). The N-nitrosodimethylamine and N-methylformamide were identified by comparison to the EPA vapor phase library spectra. The best spectral fit for the compound shown in 8c was acetamide. However, the HQI in this case was not especially low (0.4). A visual comparison of the unknown and reference spectra indicated that, although the main bands were present, significant variation in the weaker bands suggest that a different amide is more likely. The fact that these products are observed with the nitramine/borohydride mixtures but not with either component alone is significant, and shows that the decomposition of RDX and HMX is modified by the boron compounds. The N-nitrosodimethylamine is especially prominent in the decomposition products and is always present at a relatively high level.

Another significant effect of the boron is that the products shown in Figures 7a and 7b (an unknown amide and N,N-dimethylformamide) are seen only in high temperature HMX/RDX decomposition. However, with the boron materials present these are seen at both low and high temperatures. This suggests that the boron salts catalyzed the decomposition of the nitramines. Also, even in the low temperature decomposition of the boron mixtures, products shown in 4a, 4b, and 4c (R-C-N=O, formic acid and the unknown ketone) are at reduced levels, more similar to high temperature RDX/HMX decomposition. This also suggests catalysis by the boron compounds. It is also noted that, even in low temperature decomposition of the mixtures, the compound (Figure 8a) seen in high temperature decomposition of the tetramethylammonium salt is observed. This is true in mixtures in which the potassium salt or NaBH_4 is the boron

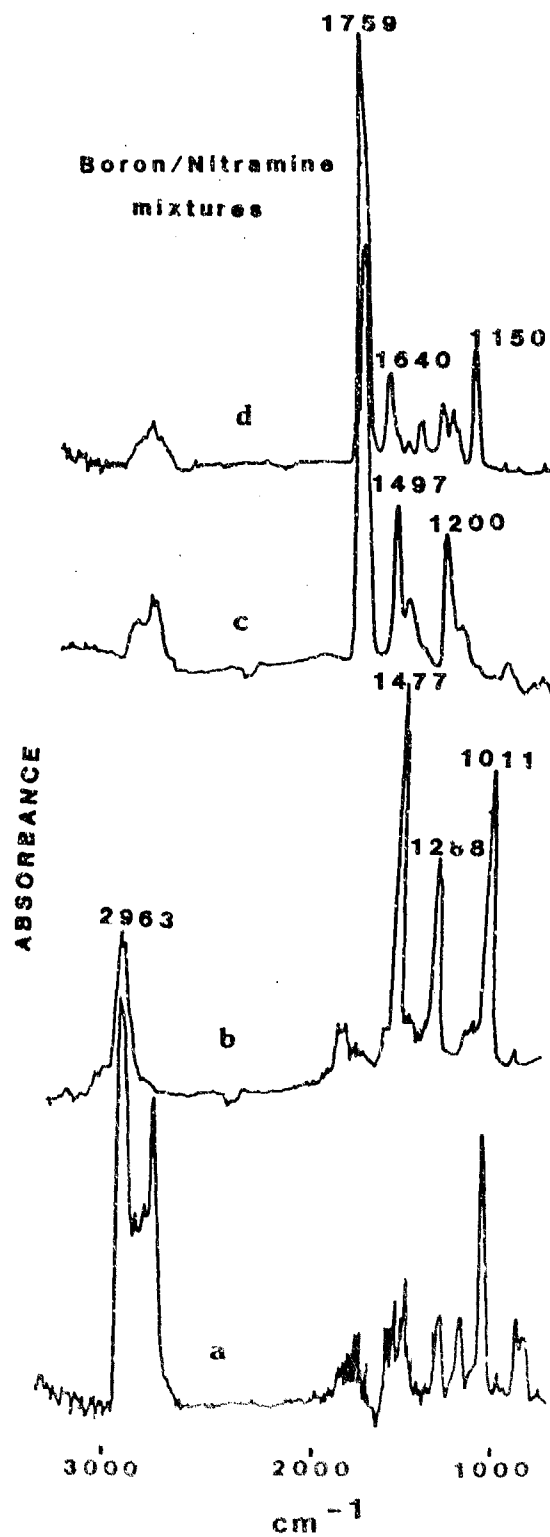


Figure 8. Infrared Spectra of Products Unique to Nitramine/Boron Mixtures. These products are generated at either low (280-320°C) or high temperatures (800°C).

source as well. Thus, the nitramine and boron salts appear to act synergistically to produce this compound. Also, the three boron materials tested seem to affect RDX decomposition in a manner such that even at low temperatures the products are more similar to those seen in high temperature decomposition. In addition, new decomposition products are observed.

The effect of boron on RDX/HMX decomposition is apparent in the above cases in which the boron compound and nitramine are present in equal quantities. However, in propellant formulations being tested in the closed bomb the quantity of the boron material is much lower, about 10-15% by weight. Thus, it was desirable to run some actual propellant formulations to determine if the lower levels of boron exert similar effects. The propellant formulations also contain a binder, in this case Kraton, which could also affect the RDX/boron reaction/interactions. Two propellants consisting of RDX, Kraton and the tetramethylammonium salt of the $B_{10}H_{10}$ anion (Table 3) were run at 280°C and 800°C. These propellant formulations were selected because closed bomb studies had been previously performed on them.¹⁰

Table 3. Formulations of the Propellants Studied by Pyrolysis-GC-FTIR, Chosen Because Previous Studies Were Performed On These Using a Closed Bomb¹⁰

Sample ID	Fuel	Percent Fuel	Oxidizer	Percent Oxidizer	Binder	Percent Binder	Theoretical Maximum Density
TC-014	H466	12.0	RDX	73.0	Kraton	15.0	95
TC-016	H466	12.0	RDX	83.0	Kraton	5.0	95

The infrared chromatograms for the low temperature decompositions are shown in Figure 9 (a and b); c is the chromatogram of the tetramethylammonium $B_{10}H_{10}$ salt/RDX mixture for comparison. Quantitative differences are apparent, due to differences in the formulations. Elution times in the two propellant/materials are slightly different due to the strong water peak (water adsorbed onto the propellant) which modifies column-solute interactions. Also, peak #1 co-elutes with water in the TC016 propellant and elutes near 7.8 in the RDX/borohydride. The water peak is missing in the RDX/borohydride since pure compounds were used.

The work shows that quantitative differences can be seen between propellants with similar formulations with this technique. The products in each case are qualitatively identical (with the exception of water) to those seen in the two-component mixes. That is, even at low temperatures, the high temperature N,N-dimethylformamide is generated, as was seen in boron/RDX mixes (Figure 8). Also, at low temperatures the products typically seen in RDX decomposition alone are not observed in the formulated propellants; this effect was also seen in RDX/borohydride hand mixtures (Figure 8). Table 4 summarizes the decomposition products found for each sample described thus far in this report. The compounds unique to the boron/RDX mixes, particularly N-nitrosodimethylamine are also generated in the propellant formulations.

FTIR Chromatograms

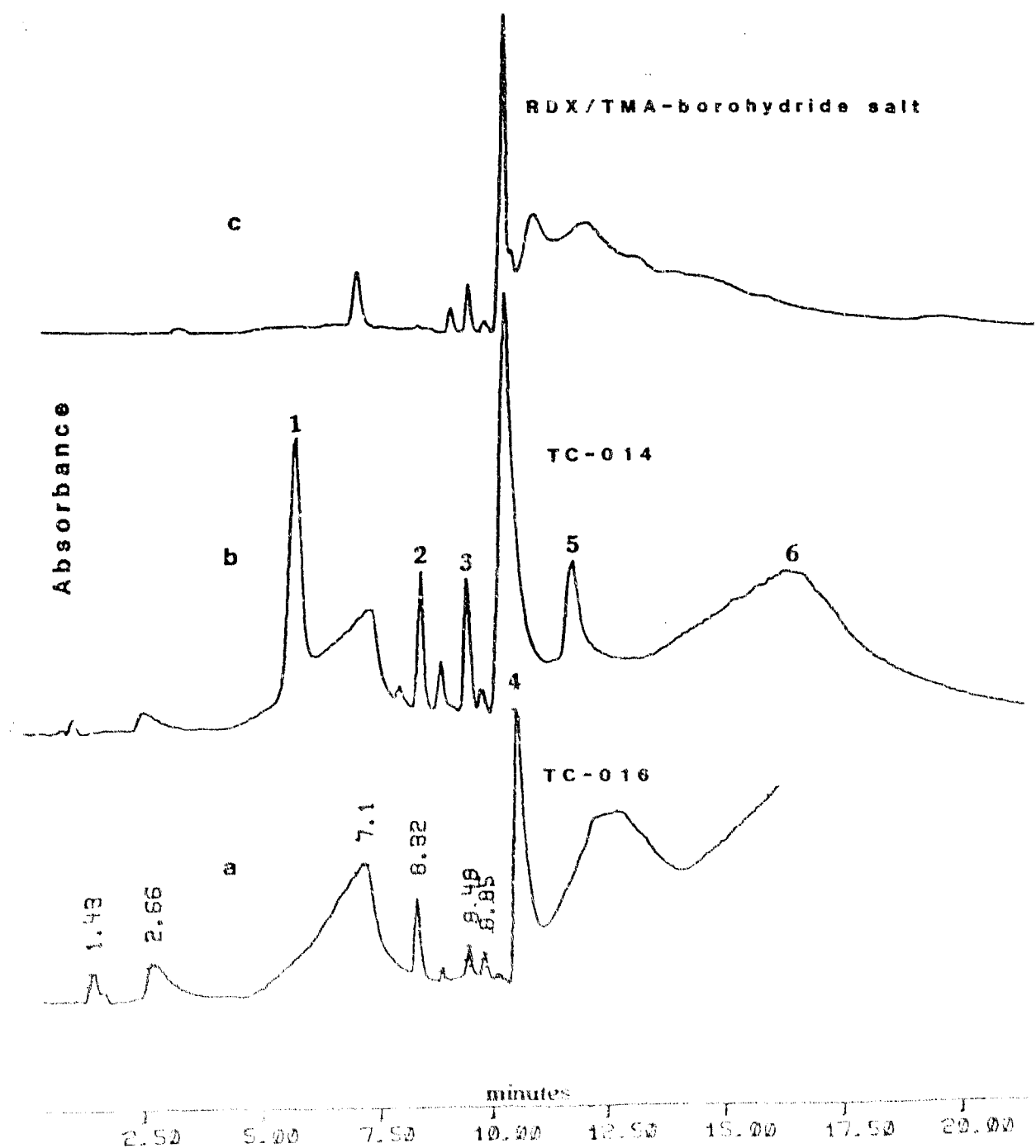


Figure 9. Infrared Chromatogram of Two Similar Propellant Formulations, TC016 (a) and TC014 (b). The result for the TMA salt/RDX mixture is shown in "c" for comparison. Peaks labeled 1 through 6 correspond to (1) $\text{C}\equiv\text{N}$, possibly cyclic functionality, (2) the decomposition product of the TMA salt, (3) *N*-Nitrosodimethylamine, (4) *N,N*-dimethylformamide, (5) *N*-methylformamide, and (6) formamide.

Table 4. Summary of Compounds Found in Each Sample Pyrolyzed and Analyzed by Capillary GC-FTIR

	A	B	C	D	E	F	G	H	I	J	K	L
RDX280	*	*	*	*	*							
RDX800	*		*	*	*	*	*					
K/RDX280	*	*	*	*			*	*	*	*		*
K/RDX800			*	*				*		*		*
M/RDX280			*	*			*	*	*	*		*
M/RDX800			*	*			*	*	*	*		*
NaBH/RDX280			*	*			*	*	*	*		*
NaBH/RDX800			*	*			*	*	*	*		*
HMX320		*	*								*	
HMX800		*	*	*			*	*			*	
K/HMX320			*	*			*	*	*			*
K/HMX800			*	*			*	*				*
M/HMX320			*				*	*	*	*		*
M/HMX800			*				*	*	*			*
TC14(280)				*								
TC14(800)			*	*			*	*	*			*
TC16(280)			*	*			*	*				*
TC16(800)			*	*				*	*			*
Triazine	*											

Letter	Compound
A	C-N=O (C-Nitroso)
B	Formic Acid
C	R-C≡N
D	Formamide
E	Ketone
F	Amide
G	N,N-Dimethylformamide
H	N-Nitrosodimethylamine
I	N-Methylformamide
J	Possible Amide
K	Possible Amide

V. PYROLYSIS PRODUCT ANALYSIS BY PACKED COLUMN CHROMATOGRAPHY

In the above work, the majority of the species isolated were compounds which would condense at ambient temperatures. Independent experiments were

performed in order to study smaller molecular weight (e.g., permanent gas) products of boron-modified nitramine decomposition. In this case samples were pyrolyzed directly into a heated GC interface and the samples retained at the head of the packed column by cryogenic cooling.

Unlike the concentrator-capillary experiments, no trap was used to collect samples during pyrolysis and the pyrolysis atmosphere (He) and flow rate was necessarily the same as that used by the GC. A Porapak column was used for the separation. Compounds larger than three to five carbon-atoms are sterically hindered and cannot pass readily. The initial temperature of the GC was subambient (-50°C) to facilitate separation of early or closely eluting species (HCN and H_2O). Some species still do not separate well including CO/NO and $\text{CO}_2/\text{N}_2\text{O}$. However, these components can be spectrally resolved since their absorptions do not overlap and therefore both qualitative and quantitative measurements can be made. As in the previous experiments, the nitramines and boron compounds were run individually first and then mixtures of each boron and nitramine were run. All samples were analyzed in duplicate and many were run in triplicate. The temperatures were the same as above, that is, 280°C for samples with RDX, 320°C for HMX and 800°C for all samples.

The gases found in each sample with nitramine present include CO_2 , N_2O , HCN, and H_2O as the major species as well as CO, NO, CH_4 , NH_3 , formaldehyde and a few products also observed in the capillary column concentrator studies. The gases generated from each sample are summarized in Table 5. The low temperature decomposition of RDX produced more N_2O than CO_2 ; formaldehyde, H_2O and HCN are also formed, however little CO, NO, CH_4 , or NH_3 was detected. A few components seen in the concentrator studies were observed, namely the C-nitroso species (Figure 4a), the suspected ketone (4e) and the C=N species (4c). The fact that no other products are seen is not surprising since the chromatographic column may exclude them. Two unidentified species are also observed (Figure 10). The product whose spectrum is shown in Figure 10b often coelutes with the C-nitroso species but was not observed in the concentrator studies.

At 800°C the product profile is significantly different. The N_2O concentration is significantly lower and the CO_2 is higher compared to those at 280°C . This is in agreement with the findings of other researchers studying nitramine decomposition.⁷ Also, very large quantities of CO and NO were evolved, whereas little was detected at the lower temperature; CH_4 is also detected at 800°C . On the other hand, formaldehyde and the ketone seen at the lower temperature are not present at the higher temperature, and the C-nitroso species is present only at a very low level. This is consistent with the results of the GC-FTIR concentrator studies which also showed a loss of these components with increasing temperatures. However, the shift in levels of CO_2 and N_2O and the increase in the amount of CO and NO with increasing temperature are new observations. The catalysis of RDX decomposition by the borohydrides may result in an increased pressure which also has an effect on the products obtained.

HMX behaves similarly in some respects to RDX, but differently in others. The N_2O to CO_2 ratio is greater at lower temperature than at higher ones, as seen with RDX. However, appreciable quantities of CO and NO are present in each case with HMX whereas little was seen for low temperature RDX pyrolysis. As with RDX, the C-nitroso and cyclic C=N compounds were observed

Table 5. Summary of Compounds Found in Each Sample Pyrolyzed and Analyzed by Packed Column GC-FTIR

	CO	NO	CO ₂	N ₂ O	CH ₄	† F ₂	H ₂ O	HCN	KRDX	NH ₃
RDX280	w	w	*	+		*	*	*		*
RDX800	*	*	+	*	*		*	*		*
K/RDX280	w	w	+	*	*		*	*		w
K/RDX800	w	w	+	*	*		*	*		w
M/RDX280	w	w	+	*			*	*		w
M/RDX800	*	w	+	*			*	*		w
NaBH/RDX280	w	*	+	*	*		*	*		w
NaBH/RDX800	*	*	+	*	*		*	*		w
HMX320	*	*	*	+			*	*	*	w
HMX800	*	*	+	*			*	*		w
K/HMX320	*	*	+	*			*	*	*	w
K/HMX800	*	*	+	*			*	*	*	w
M/HMX320	*	*	+	*			*	*	*	w
M/HMX800	*	*	+	*			*	*		w

† - Formic acid

* - Component present in decomposition products

+ - Component present in especially large quantity

w - Infrared spectral bands due to these components were weak

at low temperatures, but little or none of the C-nitroso species was present at high temperatures. Thus, as was observed in RDX, the biggest difference between low and high temperature HMX decomposition is that the ratio of N₂O to CO₂ is greater at the lower temperatures.

When mixed with the boron compounds, the biggest change in the RDX decomposition was the presence of greater quantities of CO₂ relative to N₂O, so that even at low temperatures the mixture behaves more like those at high temperatures. Also, the C-nitroso and probable ketone compound were at reduced levels (if present at all) compared to the level for low temperature RDX. This is in agreement with results obtained with the concentrator/capillary system in which the boron material seems to exert the same effect on RDX decomposition products as increasing the temperature or pressure.

VI. THERMAL ANALYSIS RESULTS

The nitramines, boron salts and nitramine/boron mixtures were also run by DSC in order to determine any effect of the boron on the temperature profile of the nitramines. The DSC of RDX alone is shown in Figure 11 in which the melting endotherm at 207°C is observed, followed immediately by a strong,

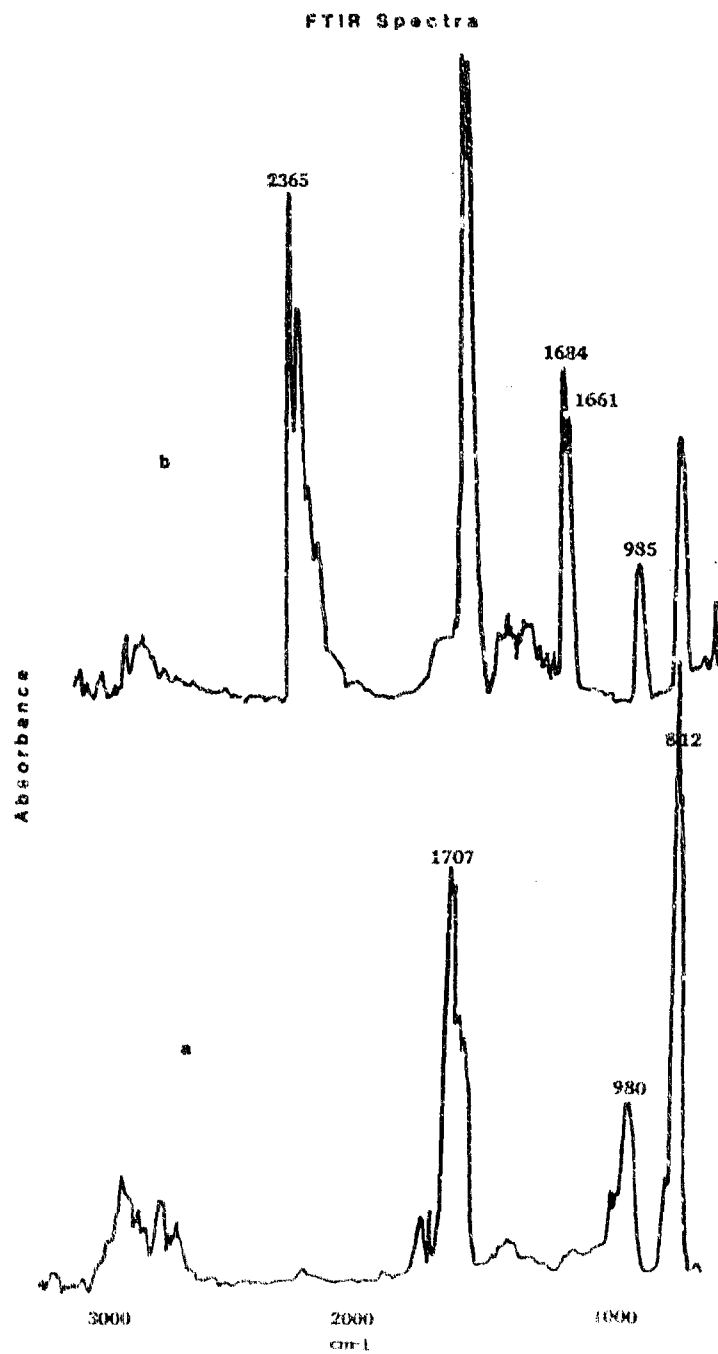


Figure 10. Infrared Spectra of Two Decomposition Products Isolated by the Packed Column Analysis and not Seen in the Concentrator-Capillary Work. The products were observed chiefly in low temperature (280°C) pyrolysis.

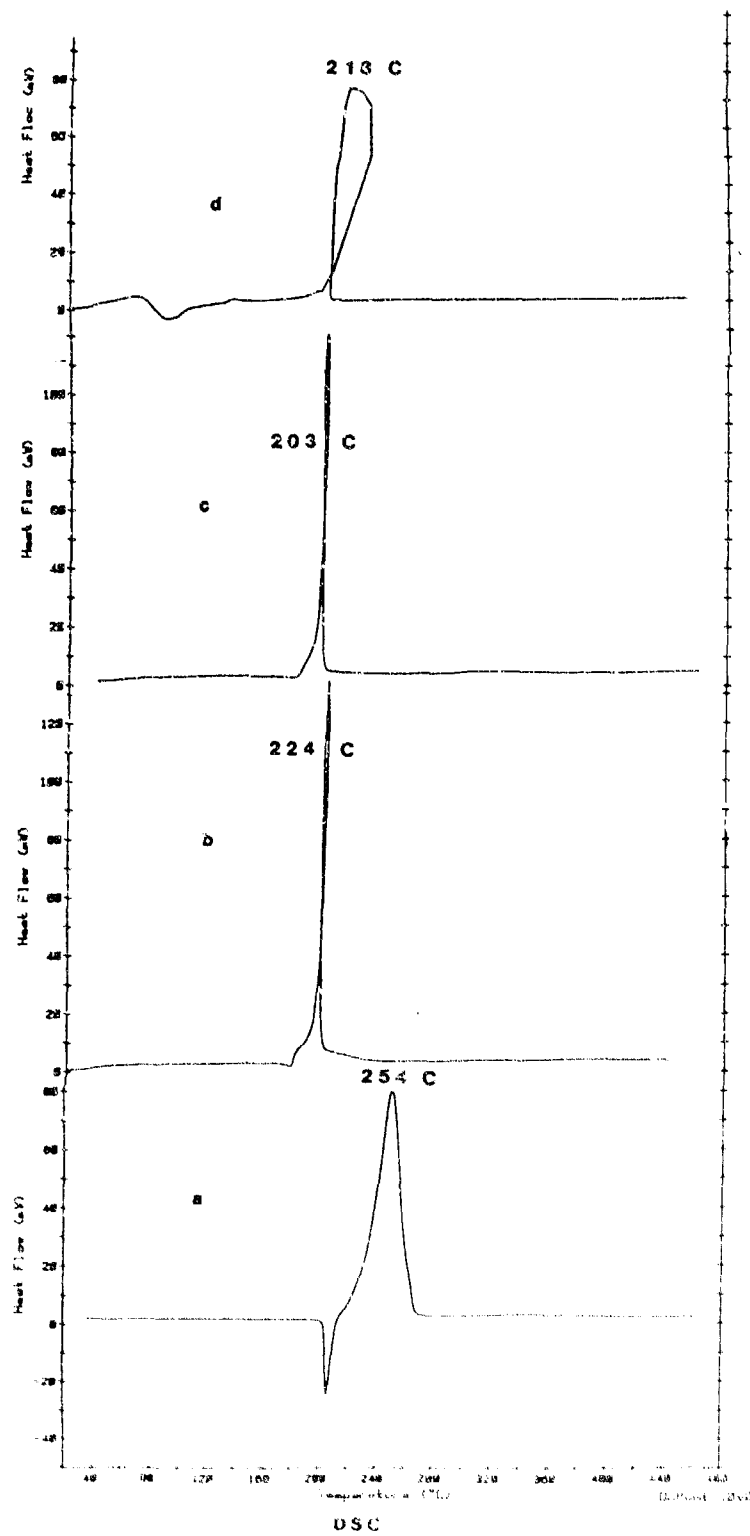


Figure 11. DSC Results for RDX (a) and Roughly 50:50 Mixtures of RDX with the Potassium Boron Salt (b), the TSA Boron Salt (c) and NaBB₆ (d)

broad decomposition exotherm at 254°C. The results with 50:50 RDX:boron mixtures are seen in 11b (potassium salt), 11c (tetramethylammonium salt) and 11d (sodium borohydride).

Two major differences are immediately apparent. The first is the shape of the exotherm for the mixtures which is much sharper in time compared to RDX alone, so sharp in fact, that there is a slight drop in temperature after the initial energy release. This occurs even though the instrument attempts to maintain its temperature program. This could happen if, after the initial sharp exotherm (heat release), the feedback control prevents further DSC heating. However, the release is quick and there is probably a delay before the heating mechanism takes over.

The second difference is the temperature of maximum decomposition which is 224°C for the potassium salt mixture, 218°C for the sodium borohydride and 203°C for the tetramethylammonium salt (about 30-50°C lower than for RDX alone). The height of the exotherms are always greater for borohydride-containing samples of comparable weight (that is, total weight, and with a 50:50 mixture, that corresponds to half the amount of RDX). Typically, peak areas which are proportional to the energy released (or absorbed) are calculated. However, the unusual shape of the RDX/boron mixture traces prevents such data analysis. Although results for 50:50 mixtures are shown here, additional experiments showed that 15-20% by weight of the salts are sufficient to obtain DSC results similar to those shown in Figure 11.

The results for the dodecahydrododecaborane salts alone are shown in Figure 12. The broad endotherm between 60 and 120°C in the case of the potassium salt (12a) is a result of decomposition as evidenced both by its weight loss (see Figure 13 below) and by a slight brownish tint which the sample acquires when heated. This endotherm is not obvious in the RDX/potassium salt mixture due to the scale needed to display the strong exotherm (Figure 11b); it is apparent however, if the ordinate axis is expanded. The tetramethylammonium salt (12b) alone is virtually unreacted near the temperature at which the RDX mixtures decompose.

Two different dodecahydrododecaborane salts (with inorganic and organic cations) produced similar effects in both pyrolysis experiments and DSC temperature profile, as did a much simpler salt, sodium borohydride. It was desirable to determine if elemental boron may produce similar effects. The results for a 50:50 mixture of RDX/elemental boron is shown in Figure 14. The trace is almost identical to that of RDX alone, with the exception of a shoulder on the high temperature side of the peak not usually seen in RDX alone. Thus, it appears that elemental boron is not sufficient to modify the decomposition of RDX in the DSC.

Since elemental boron did not exhibit any apparent modifying effect similar to the boron hydride, partially decomposed samples of the tetramethylammonium salt were analyzed in mixtures with RDX by DSC. The first sample (Figure 14) consisted of RDX mixed with the tetramethylammonium salt which had been previously decomposed at 460°C. This result is identical to the undecomposed salt, both in terms of curve shape and shift in temperature at which the RDX exotherm occurs. However, in Figure 14 is shown the result for a mixture of RDX and the 760 C-pretreated TMA salt. Not surprisingly, at this temperature the boron salt exhibits only a little of its previous

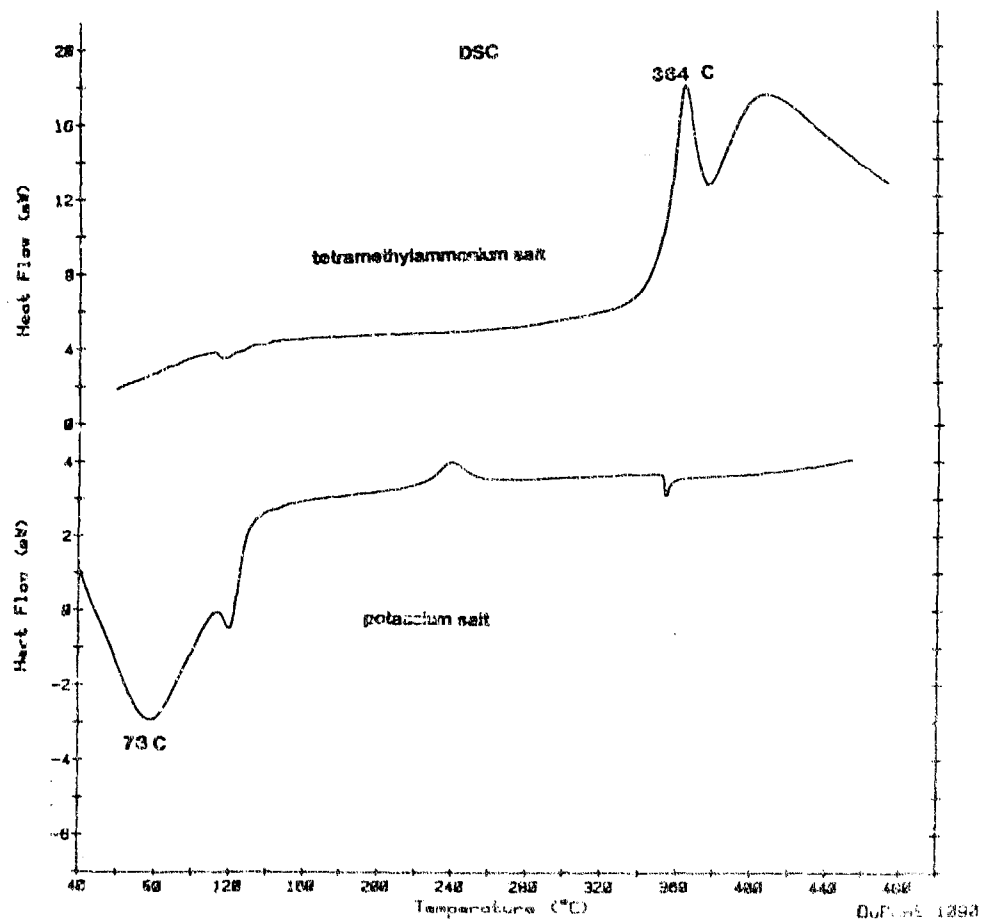


Figure 12. DSC Results for the Potassium Dodecahydrododecaborane (a) and Tetramethylammonium Dodecahydrododecaborane (b) Salts. The potassium salt is partially decomposed at the temperature at which RDX normally undergoes a decomposition exotherm whereas the tetramethylammonium salt is intact.

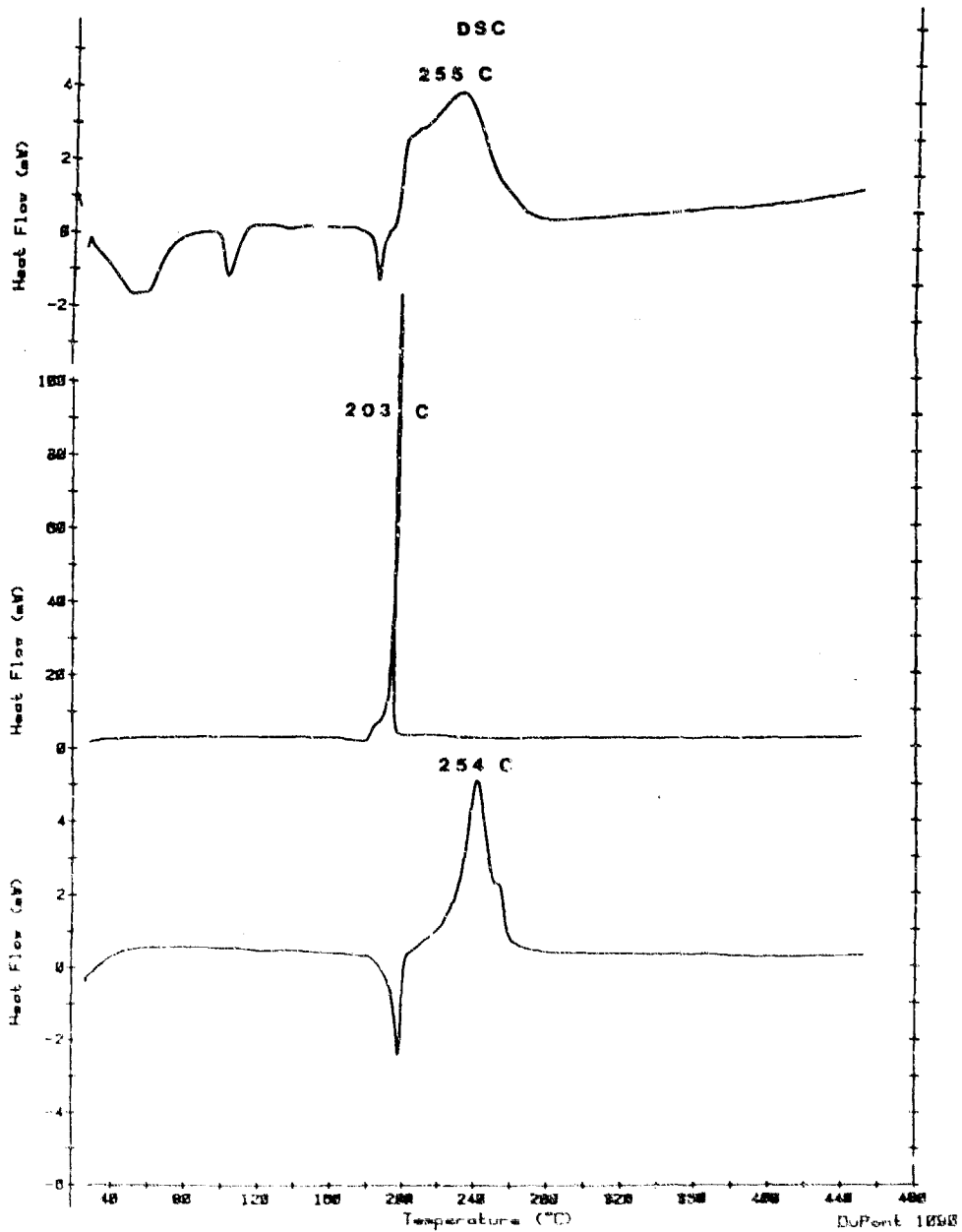


Figure 14. DSC Results for Mixtures of RDX with Elemental Boron (a), the PSA Salt Pretreated at 560°C (b) and 760°C (c)

activity. The exothermic curve is quite broad relative to the narrow endotherm seen with the undecomposed salt. However, in the mixture, the RDX exotherm begins at a lower temperature than with RDX alone; also, the melt endotherm is shifted to lower temperatures.

In Figure 13 are shown the thermogravimetric analyses between 40 to 480°C for the two $B_{12}H_{12}$ boron salts used. The potassium salt loses about 7% of its weight by 110°C and about 9.8 by 360°C. Hydrogen comprises about 5.5% of the total weight of the compound and each boron contributes about 4.9%. Assuming that the potassium remains in the residue and allowing for a conservative estimate of experimental error, at most an average of two boron atoms per molecule could be evolved by 120°C. More likely, a significant percentage of the material lost in this temperature region is hydrogen; if all hydrogens were lost from the material, the weight loss would be 5.5%; the simplest means for accounting for the 7.1% weight loss is that one boron and 10 hydrogen atoms per molecule are evolved. Of course, this assumes that all molecules undergo the same reaction in this temperature regime, which may not be true. In any case, it seems likely that most of the boron and significant quantities of potassium are not lost in this early process. Even with the probable loss of a significant portion of the hydrogen, the remaining hydride salt material is sufficient to exert the modifying effect on the RDX decomposition. It should be noted that this initial weight loss is suspiciously close to the region expected for loss of any water present in the sample; however, water loss was minimized by using dried samples. Also, the sample becomes light brown in color in this temperature range, verifying that decomposition has occurred.

The case for the tetramethylammonium salt is shown in Figure 13b. In this case, only a minimal amount of material is lost at the temperature at which RDX decomposes. However, significant decomposition (18.5% weight loss) occurs by 360°C. As discussed above, even with almost 20% of the total weight of the compound evolved, the salt still retains its modifying effect on RDX. However, this may not be too surprising since the weight loss may be mainly due to the tetramethyl functional groups. It should also be noted that the DSC sample pans are open (i.e., no lids) and that the argon purge flow through the chamber is 30 cc/min. At this flow there is little chance for evolved hot gases to collect above the sample and affect further reactions. Thus, the effects seen in this work are probably largely due to solid/liquid phase interactions.

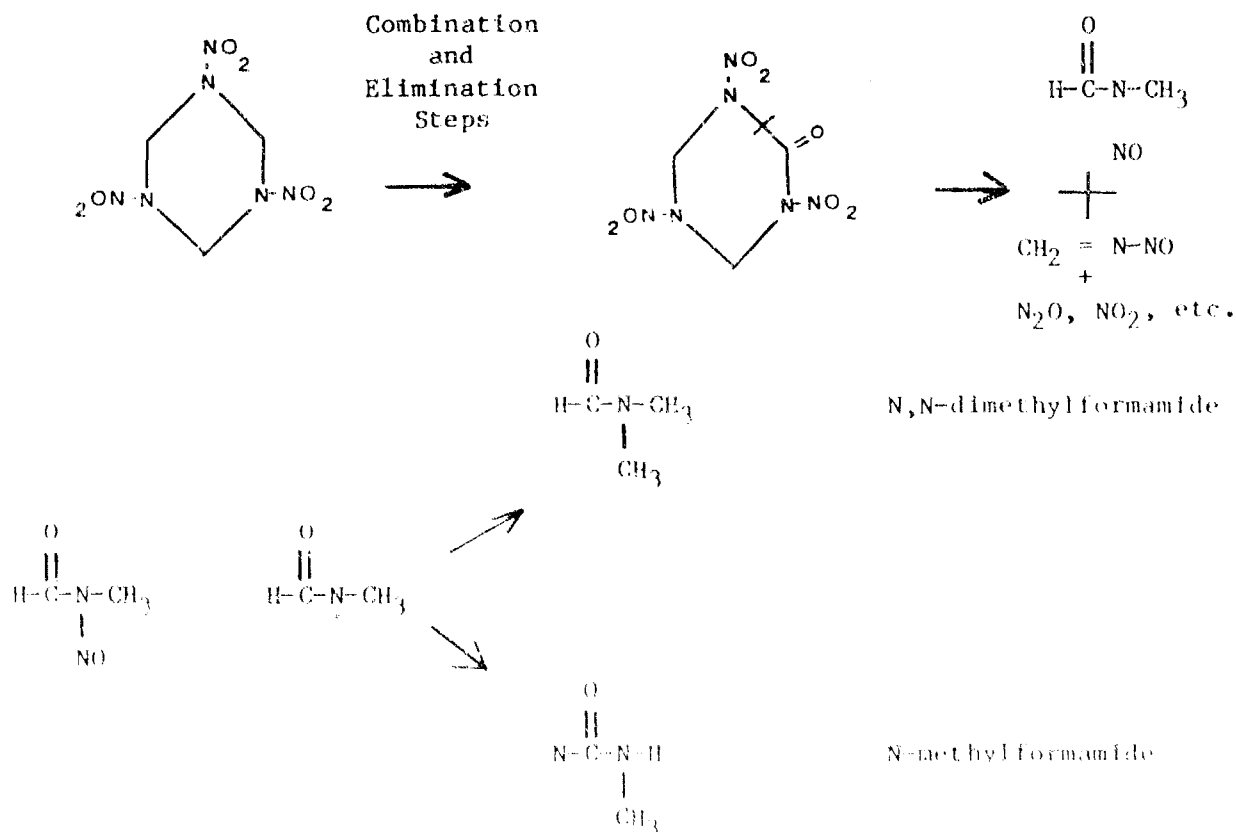
VII. DISCUSSION

The scope of this work is not primarily to determine mechanisms of nitramine decomposition, however, a brief discussion of the possibilities seems appropriate, especially in light of the types of products observed. To my knowledge, some of the products trapped in this work have not been previously seen in RDX decomposition, particularly several of the high temperature and/or boron catalyzed products such as N,N-dimethylformamide, N-nitrosodimethylamine and N-methylformamide. Also, the discovery of the C-nitroso and N-nitroso compounds this large are significant, because currently the only N-nitroso compounds to be seen have been in the solid or liquid decomposition products. Judging from the array of products observed (in this work and other work as well), it is quite likely that more than one

mechanism is involved and one can at best only speculate about what the possibilities might be. Some of the observations can be explained as follows:

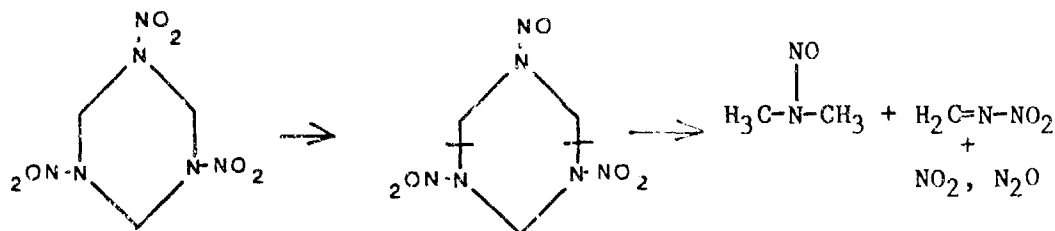
1. It was seen in the packed column studies that increasing the NO_2/CO_2 ratio is greater at lower temperatures and decreases with temperature. In preliminary experiments it was also observed that NO_2 was released at temperatures below that at which other decomposition products elute, suggesting that at low temperatures at least, N-NO_2 or HONO cleavage may be an initial step. This has been suggested by other workers who favor N-NO_2 cleavage to C-N (at low temperatures) and propose that higher temperatures may be required to achieve the energy necessary to break the C-N bond.¹¹

2. Formamide is found in every sample decomposition involving the nitramines and could possibly be due to the reaction of H_2O and HCN . However, the observation that two other amides, namely methylformamide and dimethylformamide, as well as two other compounds (quite probably amides) are present suggests some cleavage of C-N bonds in the ring. In order to form in a manner analogous to the way formamide may form (that is, condensation of water and HCN), alcohols such as methanol and ethanol would be required (instead of water) and, in high concentrations, these are not feasible reaction products of HMX/RDX . Alternative cleavages of the C-N bonds other than what has previously been proposed by others, analogous to the depolymerization of trioxane to formaldehyde may also be possible.^{12,13} In the trioxane analogy the C-N bonds of RDX are cleaved symmetrically to yield three molecules of N-nitro formimine compounds. However, if other cleavages of the type shown below are possible then the formation of the observed amides might be as follows (A):



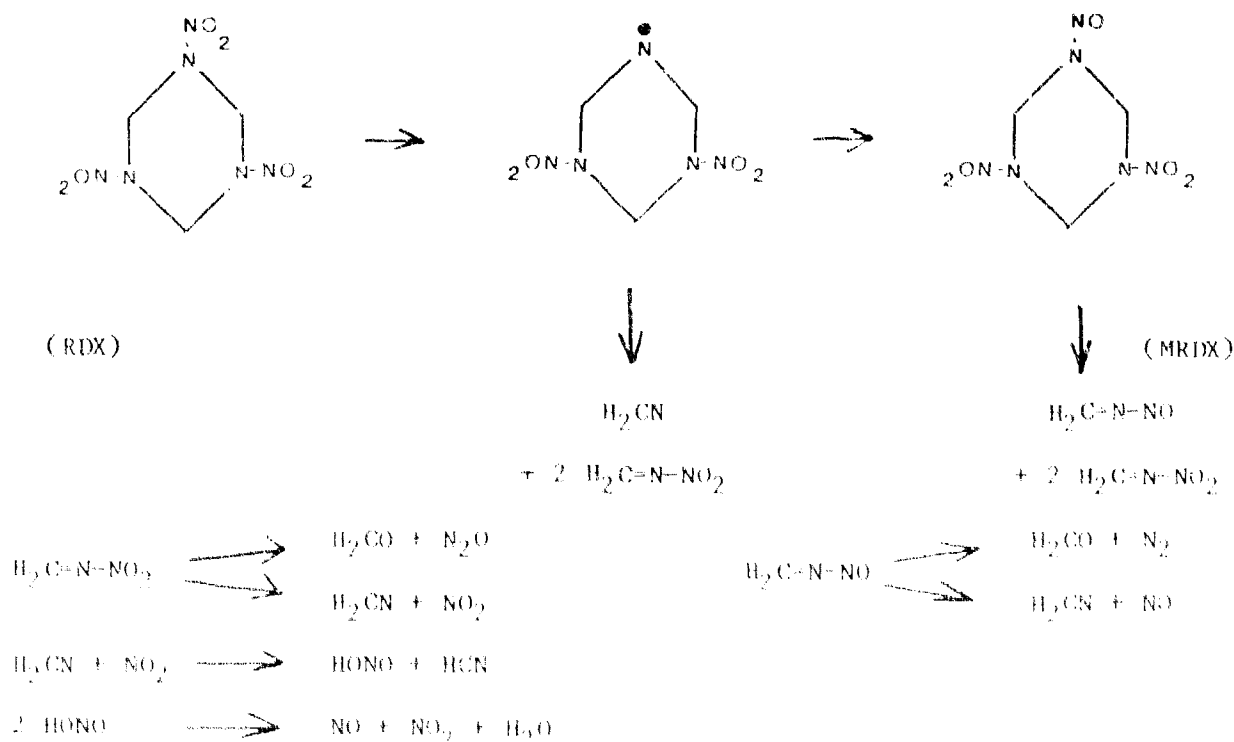
The carbonyl in the ring may seem rather unlikely. However, ketones and amides are major products of all the samples in this work and indicate that early carbonyl formation is quite probable. Also, one of the products found in many samples had an infrared spectrum quite similar to the cyclic ketone, 1-cyclopentene-3one, indicating that ring carbonyl formation may occur. Although such a 5 member ring is not likely to be formed, similar band shifts from the 6-membered ring might occur with RDX decomposition due to nitrogen in the ring.

The N-dimethylnitrosamine might be formed as follows (B):



Of course these pathways are probably not the preferred reactions (if they occur at all), but they do represent the most direct way of accounting for the observed products. It should also be noted that these products are observed only at the higher temperatures used (N,N-dimethylformamide) or in the presence of boron (N-dimethylnitrosamine and N-methylformamide), where presumably the energy content on the system might be high enough to make such reactions somewhat feasible.

One scheme proposed by other workers in our laboratory was based on the discovery of MRDX in the solid phase and also on mass spectrometric evidence reads as follows (14):



However, no exact identification of N-nitroformimine was seen in this work. In the above reference it was suggested that in Figure 4C, the probable cyclic C=N might possibly be N-nitroformimine. However, this compound was also observed in triazine (which had been dried under vacuum) pyrolysis in helium and therefore can not be N-nitroformimine (or any nitro compound), since oxygen is not available in this decomposition reaction. It may be that the formimine is produced, but not yet identified. Other products were seen which would support this mechanism include HCN, NO₂ and formaldehyde, the latter being more significant since HCN and NO can be generated by many other pathways.

It may be that any or none of the above reactions are important pathways in HMX/RDX decomposition, however, it is apparent that the reactions are quite different depending on the temperature and the presence of boron. To summarize the most significant differences:

1. Packed column results indicated that at lower temperatures the N₂O/CO₂ ratio is significantly greater than at higher temperatures.
2. Less CO and NO as well as CH₄ is observed at the lower temperatures in RDX; this effect was not as apparent in HMX. However, the temperature used for HMX may have been further along on its decomposition exotherm than was the low temperature used in the RDX studies. This is supported by the greater number of compounds detected.
3. In capillary column/concentrator studies, the C-nitroso, formic acid and probable ketone are typically observed at lower temperatures, but at lower levels than at higher temperatures (or with boron present).
4. Several high temperature products are seen in both RDX and HMX decomposition and include an unidentified amide or urea and N,N-dimethylformamide.
5. Several products seen in boron-modified reactions are not seen in RDX/HMX alone, including N-nitrosodimethylamine, N-methylformamide and an unidentified amide or ketone. These are present when either the potassium or TMA dodecahydrododecaborane salt is used, or sodium borohydride.

A few general trends include:

a. Major differences in the low and high temperature decomposition products are seen by both packed column (permanent gas analysis) and concentrator/capillary column (larger molecular weight species) analyses; the capillary and packed results seem to correspond very well.

b. Modification of the decomposition products by the boron compounds used is quite apparent. The boron salts act in two ways:

(1) They result in decomposition more similar to high (800°C) temperature ultramine decomposition, even if the mixture decomposition occurs at low temperature (280°C). That is, the typical high temperature ultramine products are seen in low temperature mixture studies. Also, products usually seen only in low temperatures in the ultramines, are not seen with boron present at low temperatures.

(2) Some products, such as N-nitrosodimethylamine, N-methylformamide and the unidentified amide or ketone are not seen at all in RDX, but are present in boron modified propellants.

Thus, the effect of boron seems to be to catalyze decomposition of the nitramines so that energy is released at a more rapid rate. Under gun and other high pressure conditions this could result in more lower molecular weight gases being produced at a faster rate. Recently instrumentation has been developed and is available to our laboratory which enables "freezing-out" of chemical products formed in a high pressure bomb. Identification of such products would provide a link between the chemistry elucidated in this work under low pressures with mechanisms most likely to occur under gun conditions. Such an understanding would be most useful in the selection of borohydride compounds for various applications in which the burning rate promotion is desired.

ACKNOWLEDGEMENT

The author would like to express sincere thanks to Leon Decker of the Ignition and Combustion Branch, Interior Ballistics Division, BRL. His support and technical assistance during the period required to set-up and perform these experiments was immeasurable and is deeply appreciated.

REFERENCES

1. A.A. Juhasz, S.T. Peters, and L.K. Asaoka, "Development of VHBR Propellant Formulations with Improved Safety Characteristics," Proceedings, 21st JANNAF Combustion Meeting, CPIA Pub. No. 412, Vol. II, pp. 333-351, October 1984.
2. R.A. Fifer, "Workshop Report: Combustion of Very High Burning Rate (VHBR) Propellants," Proceedings, 18th JANNAF Combustion Meeting, CPIA Pub. No. 347, Vol. II, pp. 45-54, October 1981.
3. R.A. Fifer and I.C. Stobie, "Combustion Thermodynamics of some Boron-Nitrogen-Hydrogen Compounds," Proceedings, 20th JANNAF Combustion Meeting, CPIA Pub. No. 383, Vol. I, pp. 611-628, October 1983.
4. R.A. Fifer and W.F. McBratney, "Catalysis of Nitramine Propellants by Metal Borohydride," BRL Memorandum Report ARBRL-MR-03300, July 1983.
5. S.A. Liebman, D.H. Ahlstrom, C.R. Foltz, C.I. Sanders, W.E. Beakes, T.C. Creighton, Proceedings, 172nd ACS National Meeting, p. 145, No. 209a, August 1976.
6. J.A. Pino, J.E. McMurray, P.C. Jurs, and B.K. Lavine, "Application of Pyrolysis/Gas Chromatography/Pattern Recognition to the Detection of Cystic Fibrosis Heterozygotes," Anal. Chem., Vol. 57, pp. 295-302, January 1985.
7. M.A. Schroeder, "Critical Analysis of Nitramine Decomposition Data: Activation Energies and Frequency Factors for HMX and RDX Decomposition," BRL Technical Report BRL-TR-2673, September 1985.
8. H.B. Woodruff and G.M. Smith, "Computer Program for the Analysis of Infrared Spectra," Anal. Chem., Vol. 52, No. 14 pp. 2321-2327, 1980.
9. The Interpretation of Infrared Vapor-Phase Infrared Spectra, Vols. I and II, Sadtler Research Laboratories, Division of Bio-Rad Laboratories, Phila. PA, 1984.
10. K.L. White, D.G. McCoy, J.O. Doall, W.P. Augst, R.E. Bowman, and A.A. Juhasz, "Closed Chamber Burning Characteristics of New VHBR Formulations," BRL-MR-3471, October 1985.
11. R. Shaw and F.E. Walker, "Estimated Kinetics and Thermochemistry of Some Initial Unimolecular Reactions in the Thermal Decomposition of 1,3,5,7-Tetrahydro-1,3,5,7-Tetraazepentane in the Gas Phase," J. Phys. Chem., Vol. 81, pp. 2572-2579, 1977.
12. S.W. Benson and H.E. O'Neal, "Kinetic Data on Gas Phase Unimolecular Reactions," NBSRDS NBS-21, p. 31411, Superintendent of Documents, US Printing Office, Washington, DC, February 1970.
13. S.W. Benson, "Thermochemical Kinetics," Wiley-Interscience, New York, p. 117, 1976.

14. R.A. Fifer, S.A. Liebman, P.J. Duff, K.D. Fickie, and M.A. Schroeder, "Thermal Degradation Mechanisms of Nitramine Propellants," Proceedings, 22nd JANNAF Combustion Meeting, CPIA Pub. No. 432, Vol. II, pp. 537-546, October 1985.

LIST OF ACRONYMS

DSC	Differential Scanning Calorimetry
FID	Flame Ionization Detector
FTIR	Fourier Transform Infrared
FSOT	Fused Silica Open Tubular
GC	Gas Chromatograph
HQI	Hit Quality Index
HMX	Cyclotetramethylene Tetranitramine
mRDX	Mononitroso Cyclotrimethylene Trinitramine
RDX	Cyclotrimethylene Trinitramine
TAGN	Triaminoguanidine Nitrate
TCD	Thermal Conductivity Detector
TGA	Thermal Gravimetric Analysis
TMA	Tetramethylammonium
VHBR	Very High Burning Rate

DISTRIBUTION LIST

<u>No. Of Copies</u>	<u>Organization</u>	<u>No. Of Copies</u>	<u>Organization</u>
12	Administrator Defense Technical Info Center ATTN: DTIC-DDA Cameron Station Alexandria, VA 22304-6145	1	Commander US Army Aviation Systems Command ATTN: AMSAV-DACL 4300 Goodfellow Blvd. St. Louis, MO 63120-1798
1	HQ EA (SARD-TR) Washington, DC 20310	1	Director US Army Aviation Research and Technology Activity Ames Research Center Moffett Field, CA 94035-1099
1	Commander US Army Materiel Command ATTN: AMCDRA-ST 5001 Eisenhower Avenue Alexandria, VA 22333-0001	4	Commander US Army Research Office ATTN: R. Ghirardelli D. Mann K. Singleton R. Shaw P.O. Box 12211 Research Triangle Park, NC 27709-2211
1	Commander US Army Laboratory Command ATTN: AMSLC-TD Adelphi, MD 20783-1145	1	Commander US Army Communications - Electronics Command ATTN: AMSEL-ED Fort Monmouth, NJ 07703
1	Commander Armament R&D Center US Army AMCCOM ATTN: SMCAR-MSI Picatinny Arsenal, NJ 07806-5000	2	Commander Armament R&D Center US Army AMCCOM ATTN: SMCAR-LCA-G, D.S. Downs J.A. Lannon Dover, NJ 07801
1	Commander Armament R&D Center US Army AMCCOM ATTN: SMCAR-TDC Picatinny Arsenal, NJ 07806-5000	1	Commander Armament R&D Center US Army AMCCOM ATTN: SMCAR-LC-G, L. Harris Dover, NJ 07801
1	Director Benet Weapons Laboratory Armament R&D Center US Army AMCCOM ATTN: SMCAR-LCB-TL Watervliet, NY 12189-4050		
1	Commander US Army Armament, Munitions and Chemical Command ATTN: SMCAR-ESP-L Rock Island, IL 61299-7300		

DISTRIBUTION LIST

<u>No. Of Copies</u>	<u>Organization</u>	<u>No. Of Copies</u>	<u>Organization</u>
1	Commander Armament R&D Center US Army AMCCOM ATTN: SMCAR-SCA-T, L. Stiefel Dover, NJ 07801	1	Office of Naval Research Department of the Navy ATTN: R.S. Miller, Code 432 800 N. Quincy Street Arlington, VA 22217
2	Commander US Army Missile Command ATTN: AMSMI-RD AMSMI-AS Redstone Arsenal, AL 35898-5000	1	Commander Naval Air Systems Command ATTN: J. Ramnarace, AIR-54111C Washington, DC 20360
2	Commander US Army Missile Command ATTN: AMSMI-RK, D.J. Ifshin W. Wharton Redstone Arsenal, AL 35898	2	Commander Naval Ordnance Station ATTN: C. Irish P.L. Stang, Code 515 Indian Head, MD 20640
1	Commander US Army Missile Command ATTN: AMSMI-RKA, A.R. Maykut Redstone Arsenal, AL 35898-5249	1	Commander Naval Surface Weapons Center ATTN: J.L. East, Jr., G-23 Dahlgren, VA 22448-5000
1	Commander US Army Tank Automotive Cnd ATTN: AMSTA-DI Warren, MI 48090	2	Commander Naval Surface Weapons Center ATTN: R. Bernecker, R-13 G.B. Wilmot, R-16 Silver Spring, MD 20902-5000
1	Director US Army TRADOC Analysis Cnd ATTN: ATAA-SL White Sands Missile Range, NM 88002-5502	5	Commander Naval Research Laboratory ATTN: M.C. Lin J. McDonald E. Oran J. Shnur R.J. Doyle, Code 6110 Washington, DC 20375
1	Commandant US Army Infantry School ATTN: ATSH-CD-CSO-OR Fort Benning, GA 31905-5400	1	Commanding Officer Naval Underwater Systems Center Weapons Dept. ATTN: R.S. Lazar/Code 36301 Newport, RI 02840
1	Commander US Army Development and Employment Agency ATTN: MODE-ORO Fort Lewis, WA 98433-5000	1	Superintendent Naval Postgraduate School Dept. of Aeronautics ATTN: D.W. Netzer Monterey, CA 93940

DISTRIBUTION LIST

<u>No. Of Copies</u>	<u>Organization</u>	<u>No. Of Copies</u>	<u>Organization</u>
4	AFRPL/DY, Stop 24 ATTN: R. Corley R. Geisler J. Levine D. Weaver Edwards AFB, CA 93523-5000	1	Applied Combustion Technology, Inc. ATTN: A.M. Varney P.O. Box 17885 Orlando, FL 32860
1	AFRPL/MKPB, Stop 24 ATTN: B. Goshgarian Edwards AFB, CA 93523-5000	2	Applied Mechanics Reviews The American Society of Mechanical Engineers ATTN: R.E. White A.B. Wenzel 345 E. 47th Street New York, NY 10017
1	AFOSR ATTN: J.M. Tishkoff Bolling Air Force Base Washington, DC 20332	1	Atlantic Research Corp. ATTN: M.K. King 5390 Cherokee Avenue Alexandria, VA 22314
1	Air Force Armament Laboratory ATTN: AFATL/DLODL Eglin AFB, FL 32542-5000	1	Atlantic Research Corp. ATTN: R.H.W. Waesche 7511 Wellington Road Gainesville, VA 22065
1	AFWL/SUL Kirtland AFB, NM 87117	1	AVCO Everett Rsch. Lab. Div. ATTN: D. Stickler 2385 Revere Beach Parkway Everett, MA 02149
1	NASA Langley Research Center Langley Station ATTN: C.B. Northam/MS 168 Hampton, VA 23365	1	Battelle Memorial Institute Tactical Technology Center ATTN: J. Huggins 505 King Avenue Columbus, OH 43201
4	National Bureau of Standards ATTN: J. Hastie M. Jacox T. Kashiwagi H. Semerjian US Department of Commerce Washington, DC 20234	1	Cohen Professional Services ATTN: N.S. Cohen 141 Channing Street Redlands, CA 92373
1	OSD/SDIO/UST ATTN: L.H. Caveny Pentagon Washington, DC 20301-7100	1	Exxon Research & Eng. Co. ATTN: A. Dean Route 22E Annandale, NJ 08801
1	Aerojet Solid Propulsion Co. ATTN: P. Michell Sacramento, CA 95813		

DISTRIBUTION LIST

<u>No. Of</u> <u>Copies</u>	<u>Organization</u>	<u>No. Of</u> <u>Copies</u>	<u>Organization</u>
1	Ford Aerospace and Communications Corp. DIVAD Division Div. Hq., Irvine ATTN: D. Williams Main Street & Ford Road Newport Beach, CA 92663	1	Honeywell, Inc. Government and Aerospace Products ATTN: D.E. Broden/ MS MN50-2000 600 2nd Street NE Hopkins, MN 55343
1	General Applied Science Laboratories, Inc. 77 Raynor Avenue Ronkonkama, NY 11779-6649	1	IBM Corporation ATTN: A.C. Tam Research Division 5600 Cottle Road San Jose, CA 95193
1	General Electric Armament & Electrical Systems ATTN: M.J. Bulman Lakeside Avenue Burlington, VT 05401	1	IIT Research Institute ATTN: R.F. Remaly 10 West 35th Street Chicago, IL 60616
1	General Electric Company 2352 Jade Lane Schenectady, NY 12309	2	Director Lawrence Livermore National Laboratory ATTN: C. Westbrook M. Costantino P.O. Box 808 Livermore, CA 94550
1	General Electric Ordnance Systems ATTN: J. Mandzy 100 Plastics Avenue Pittsfield, MA 01203	1	Lockheed Missiles & Space Co. ATTN: George Lo 3251 Hanover Street Dept. 52-35/B204/2 Palo Alto, CA 94304
2	General Motors Rsch Labs Physics Department ATTN: T. Sloan R. Teets Warren, MI 48090	1	Los Alamos National Lab ATTN: B. Nichols T7, MS-B284 P.O. Box 1663 Los Alamos, NM 87545
2	Hercules, Inc. Allegany Ballistics Lab. ATTN: R.R. Miller E.A. Yount P.O. Box 210 Cumberland, MD 21501	1	National Science Foundation ATTN: A.B. Harvey Washington, DC 20550
1	Hercules, Inc. Bacchus Works ATTN: E.P. McCarty P.O. Box 98 Magna, UT 84044	1	Olin Corporation Smokeless Powder Operations ATTN: V. McDonald P.O. Box 222 St. Marks, FL 32355

DISTRIBUTION LIST

<u>No. Of Copies</u>	<u>Organization</u>	<u>No. Of Copies</u>	<u>Organization</u>
1	Paul Gough Associates, Inc. ATTN: P.S. Gough 1048 South Street Portsmouth, NH 03801	1	Stevens Institute of Tech. Davidson Laboratory ATTN: R. McAlevy, III Hoboken, NJ 07030
2	Princeton Combustion Research Laboratories, Inc. ATTN: M. Summerfield N.A. Messina 475 US Highway One Monmouth Junction, NJ 08852	1	Textron, Inc. Bell Aerospace Co. Division ATTN: T.M. Ferger P.O. Box 1 Buffalo, NY 14240
1	Hughes Aircraft Company ATTN: T.E. Ward 8433 Fallbrook Avenue Canoga Park, CA 91303	1	Thiokol Corporation Elkton Division ATTN: W.N. Brundige P.O. Box 241 Elkton, MD 21921
1	Rockwell International Corp. Rocketdyne Division ATTN: J.E. Flanagan/HBGL 6633 Canoga Avenue Canoga Park, CA 91304	1	Thiokol Corporation Huntsville Division ATTN: R. Glick Huntsville, AL 35807
4	Sandia National Laboratories Combustion Sciences Dept. ATTN: R. Cattolica S. Johnston P. Mattern D. Stephenson Livermore, CA 94550	3	Thiokol Corporation Wasatch Division ATTN: S.J. Bennett P.O. Box 524 Brigham City, UT 84302
1	Science Applications, Inc. ATTN: R.B. Edelman 23146 Cumorah Crest Woodland Hills, CA 91364	1	TRW ATTN: M.S. Chou MSRI-1016 1 Parke Redondo Beach, CA 90278
1	Science Applications, Inc. ATTN: H.S. Pergament 1100 State Road, Bldg. N Princeton, NJ 08540	1	United Technologies ATTN: A.C. Eckbreth East Hartford, CT 06108
3	SRI International ATTN: G. Smith D. Crosley D. Golden 333 Ravenswood Avenue Menlo Park, CA 94025	3	United Technologies Corp. Chemical Systems Division ATTN: R.S. Brown T.D. Myers (2 copies) P.O. Box 50015 San Jose, CA 95150-0015

DISTRIBUTION LIST

<u>No. Of Copies</u>	<u>Organization</u>	<u>No. Of Copies</u>	<u>Organization</u>
1	Universal Propulsion Company ATTN: H.J. McSpadden Black Canyon Stage 1 Box 1140 Phoenix, AZ 85029	2	University of Southern California Dept. of Chemistry ATTN: S. Benson C. Wittig Los Angeles, CA 90007
1	Veritay Technology, Inc. ATTN: E.B. Fisher 4845 Millersport Highway P.O. Box 305 East Amherst, NY 14051-0305	1	Case Western Reserve Univ. Div. of Aerospace Sciences ATTN: J. Tien Cleveland, OH 44135
1	Brigham Young University Dept. of Chemical Engineering ATTN: M.W. Beckstead Provo, UT 84601	1	Cornell University Department of Chemistry ATTN: T.A. Cool Baker Laboratory Ithaca, NY 14853
1	California Institute of Tech. Jet Propulsion Laboratory ATTN: MS 125/159 4800 Oak Grove Drive Pasadena, CA 91103	1	Univ. of Dayton Rsch Inst. ATTN: D. Campbell AFRFL/PAP Stop 24 Edwards AFB, CA 93523
1	California Institute of Technology ATTN: F.E.C. Culick/ MC 301 46 204 Karman Lab. Pasadena, CA 91125	1	University of Florida Dept. of Chemistry ATTN: J. Winefordner Gainesville, FL 32611
1	University of California, Berkeley Mechanical Engineering Dept. ATTN: J. Daily Berkeley, CA 94720	3	Georgia Institute of Technology School of Aerospace Engineering ATTN: E. Price W.C. Strahle B.T. Zinn Atlanta, GA 30332
1	University of California Los Alamos Scientific Lab. P.O. Box 1663, Mail Stop B216 Los Alamos, NM 87545	1	University of Illinois Dept. of Mech. Eng. ATTN: H. Krier 144MEB, 1206 W. Green St. Urbana, IL 61801
2	University of California, Santa Barbara Quantum Institute ATTN: K. Schofield M. Steinberg Santa Barbara, CA 93106	1	Johns Hopkins University/APL Chemical Propulsion Information Agency ATTN: T.W. Christian Johns Hopkins Road Laurel, MD 20707

DISTRIBUTION LIST

<u>No. Of Copies</u>	<u>Organization</u>	<u>No. Of Copies</u>	<u>Organization</u>
1	University of Michigan Gas Dynamics Lab Aerospace Engineering Bldg. ATTN: G.M. Faeth Ann Arbor, MI 48109-2140	1	Purdue University Department of Chemistry ATTN: E. Grant West Lafayette, IN 47906
1	University of Minnesota Dept. of Mechanical Engineering ATTN: E. Fletcher Minneapolis, MN 55455	2	Purdue University School of Mechanical Engineering ATTN: N.M. Laurendeau S.N.B. Murthy TSPC Chaffee Hall West Lafayette, IN 47906
3	Pennsylvania State University Applied Research Laboratory ATTN: K.K. Kuo H. Palmer M. Micci University Park, PA 16802	1	Rensselaer Polytechnic Inst. Dept. of Chemical Engineering ATTN: A. Fontijn Troy, NY 12181
1	Pennsylvania State University Dept. of Mechanical Engineering ATTN: V. Yang University Park, PA 16802	1	Stanford University Dept. of Mechanical Engineering ATTN: R. Hanson Stanford, CA 94305
1	Polytechnic Institute of NY Graduate Center ATTN: S. Lederman Route 110 Farmingdale, NY 11735	1	University of Texas Dept. of Chemistry ATTN: W. Gardiner Austin, TX 78712
2	Princeton University Forrestal Campus Library ATTN: K. Brezinsky I. Glassman P.O. Box 710 Princeton, NJ 08540	1	University of Utah Dept. of Chemical Engineering ATTN: G. Flandro Salt Lake City, UT 84112
1	Princeton University MAE Dept. ATTN: F.A. Williams Princeton, NJ 08544	1	Virginia Polytechnic Institute and State University ATTN: J.A. Schetz Blacksburg, VA 24061
1	Purdue University School of Aeronautics and Astronautics ATTN: J.R. Osborn Grissom Hall West Lafayette, IN 47906	1	Commandant USAFAS ATTN: ATSF-TSM-CN Fort Sill, OK 73503-5600
		1	F.J. Seiler Research Lab (AFSC) ATTN: S.A. Shakeford USAF Academy, CO 80840-5528

DISTRIBUTION LIST

No. of
Copies Organization

Aberdeen Proving Ground

Dir, USAMSAA
 ATTN: AMXSY-D
 AMXSY-MP, H. Cohen
Cdr, USATECOM
 ATTN: AMSTE-TO-F
Cdr, CRDEC, AMCCOM
 ATTN: SMCCR-RSP-A
 SMCCR-MU
 SMCCR-SPS-IL

USER EVALUATION SHEET/CHANGE OF ADDRESS

This laboratory undertakes a continuing effort to improve the quality of the reports it publishes. Your comments/answers below will aid us in our efforts.

1. Does this report satisfy a need? (Comment on purpose, related project, or other area of interest for which the report will be used.) _____

2. How, specifically, is the report being used? (Information source, design data, procedure, source of ideas, etc.) _____

3. Has the information in this report led to any quantitative savings as far as man-hours or dollars saved, operating costs avoided, or efficiencies achieved, etc? If so, please elaborate. _____

4. General Comments. What do you think should be changed to improve future reports? (Indicate changes to organization, technical content, format, etc.) _____

BRL Report Number _____ Division Symbol _____

Check here if desire to be removed from distribution list. _____

Check here for address change. _____

Current address: Organization _____
Address _____

-----FOLD AND TAPE CLOSED-----

Director
U.S. Army Ballistic Research Laboratory
ATTN: SLCBR DD-T (NEI)
Aberdeen Proving Ground, MD 21005-5066



NO POSTAGE
NECESSARY
IF MAILED
IN THE
UNITED STATES

OFFICIAL BUSINESS
PENALTY FOR PRIVATE USE \$300

BUSINESS REPLY LABEL
FIRST CLASS PERMIT NO. 17067 WASHINGTON D.C.

POSTAGE WILL BE PAID BY DEPARTMENT OF THE ARMY



Director
U.S. Army Ballistic Research Laboratory
ATTN: SLCBR DD-T (NEI)
Aberdeen Proving Ground, MD 21005-5066

Director
U.S. Army Ballistic Research Laboratory
ATTN: SLCHR-DD-T (NEI)
Aberdeen Proving Ground, MD 21005-5066

- PASTE LABEL HERE -